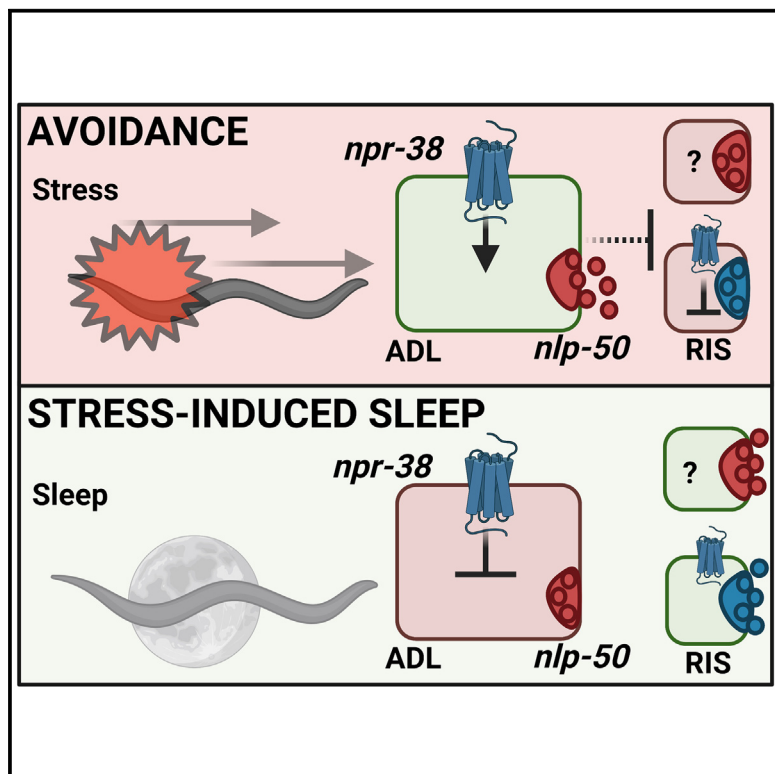


The neuropeptide receptor *npr-38* regulates avoidance and stress-induced sleep in *Caenorhabditis elegans*

Graphical abstract



Authors

Emily Le, Teagan McCarthy,
Madison Honer, Caroline E. Curtin,
Jonathan Fingerut, Matthew D. Nelson

Correspondence

mnelson@sju.edu

In brief

Sleep promotes recovery from injury or illness; however, it renders animals vulnerable to threats. The mechanisms that regulate transitions between threat avoidance and sleep are not well understood. Le, McCarthy, et al. describe a G-protein-coupled receptor, *npr-38*, that is required in the ADL sensory neurons for avoidance and sleep in *Caenorhabditis elegans*.

Highlights

- *npr-38* is required for sleep, avoidance, and general arousal
- *npr-38* is required in the ADL sensory neurons for sleep and avoidance
- *npr-38* is required in the RIS and DVA interneurons for arousal
- The ADL neurons express *nlp-50* neuropeptides which are required for sleep

Article

The neuropeptide receptor *npr-38* regulates avoidance and stress-induced sleep in *Caenorhabditis elegans*

Emily Le,^{1,2} Teagan McCarthy,^{1,2} Madison Honer,¹ Caroline E. Curtin,¹ Jonathan Fingerut,¹ and Matthew D. Nelson^{1,3,*}

¹Department of Biology, Saint Joseph's University, Philadelphia, PA 19131, USA

²These authors contributed equally

³Lead contact

*Correspondence: mnelson@sju.edu

<https://doi.org/10.1016/j.cub.2023.06.042>

SUMMARY

Although essential and conserved, sleep is not without its challenges that must be overcome; most notably, it renders animals vulnerable to threats in the environment. Infection and injury increase sleep demand, which dampens sensory responsiveness to stimuli, including those responsible for the initial insult. Stress-induced sleep in *Caenorhabditis elegans* occurs in response to cellular damage following noxious exposures the animals attempted to avoid. Here, we describe a G-protein-coupled receptor (GPCR) encoded by *npr-38*, which is required for stress-related responses including avoidance, sleep, and arousal. Overexpression of *npr-38* shortens the avoidance phase and causes animals to initiate movement quiescence and arouse early. *npr-38* functions in the ADL sensory neurons, which express neuropeptides encoded by *nlp-50*, also required for movement quiescence. *npr-38* regulates arousal by acting on the DVA and RIS interneurons. Our work demonstrates that this single GPCR regulates multiple aspects of the stress response by functioning in sensory and sleep interneurons.

INTRODUCTION

Sleep may occur in all animals, yet the function of sleep is debated. Its ubiquitous presence suggests ancient and essential benefits¹ such as energy conservation,² metabolic compartmentalization,³ memory consolidation,⁴ and recovery from injury or illness.⁵ These advantages have preserved sleep throughout evolution, despite its inherent disadvantages. Sleep prevents detection and escape from threats and limits food-seeking and reproduction.⁶ Animals must therefore coordinate sleep with behaviors required for their survival; the mechanisms underlying this balance are, however, unclear.

Although sleep is a periodic event controlled by a molecular clock,⁷ it can be induced independently of circadian regulation. Sleep can be initiated in response to cellular damage, also known as stress-induced sleep.^{8,9} The stress response of the nematode *Caenorhabditis elegans* comprises two essential behavioral states: threat avoidance and a subsequent recovery sleep called stress-induced sleep.^{8,10} Animals attempt to escape threats such as pathogens,¹¹ extreme temperatures,^{12,13} and ultraviolet (UV) light^{14,15} via a reflexive mechanism executed by sensorimotor systems.¹¹ Following escape, if cellular damage has incurred, sleep is induced to facilitate restorative pathways.^{5,16} The downside of this sleep is that it renders animals less responsive to the initial threat. How escape and stress-induced sleep are coordinated at the molecular level is unknown.

The mechanisms of avoidance and sensorimotor integration have been well characterized. Although sleeping animals have

an elevated arousal threshold,^{8,17} their sensory neurons are still capable of detecting noxious stimuli. Warming temperatures are detected by the ADL,¹⁸ AFD, and FLP neurons,^{13,19} whereas noxious UV irradiation is detected by the ASH and ASJ sensory neurons.^{20,21} Heat avoidance and arousal from sleep require the hub interneuron RMG,^{22–24} which is necessary for the accelerated movements that are characteristic of an escape response.²⁵ Considering that both the escape and sleep responses are essential and at odds with each other, animals must coordinate the timing of these behaviors.

Upon exposure to damaging stimuli, movement quiescence appears to be suppressed until the noxious stimulus is removed, suggesting that escape circuits override those promoting quiescence of movement. Stress-induced sleep requires components of epidermal growth factor (EGF) signaling. The EGF receptor *let-23*²⁶ is required in two sleep-promoting interneurons, the ALA²⁷ and RIS.²⁸ The ALA expresses neuropeptide-like proteins (*nlp*), such as *nlp-14*,²⁹ and FMRFamide-related peptides (*flp*),^{30,31} which have been shown to function in sleep by inhibiting wake behaviors and sensory arousal.³⁰ RIS expresses *flp-11* peptides, which can inhibit movement,^{28,32,33} and this movement quiescence requires the inhibition of wake-active interneurons, such as the DVA, which function downstream.³⁴ The mechanisms that underlie the transition between avoidance and sleep are unknown.

We hypothesized that the orcoxinin-like *nlp-14* neuropeptides regulate both behavioral states, considering that *nlp-14* mutants initiate premature movement quiescence.²⁹ *nlp-14* mutants

enter a sleep state 15–30 min earlier than wild-type controls, whereas displaying an overall reduced amount of total movement quiescence.²⁹ To explore this further, we conducted a forward genetic suppressor screen of animals overexpressing *nlp-14*, which causes quiescence of movement and prolongs the rhythmic defecation cycle.²⁹ We isolated a strain possessing a putative loss-of-function allele (*stj330*) of the gene *npr-38* (T10E10.3), which encodes an orphaned neuropeptide G-protein-coupled receptor (GPCR).³⁵ *npr-38* is expressed in the aforementioned ADL, ASH, and RMG neurons; the sleep-regulating ALA²⁷ and RIS³⁶ as well as the wake-promoting DVA.³⁴ We find that *npr-38* regulates multiple aspects of the stress response, including avoidance, sleep, and arousal. Our data support a model in which *npr-38* promotes movement during wakefulness via the RIS and DVA interneurons. Upon stress exposure, *npr-38* regulates avoidance and stress-induced sleep by acting primarily on the ADL sensory neurons, which are synaptically connected to the ALA and RIS. The ADL neurons express *nlp-50* neuropeptides, which are required for sleep and can promote arousal when overexpressed. Our data suggest that *npr-38* regulates multiple aspects of the stress response by modulating the activity of sensory and sleep/wake interneurons.

RESULTS

npr-38 encodes a GPCR that is required for *nlp-14*-induced sleep

To identify genes that control stress-induced sleep, we focused on the *nlp-14* pathway. *nlp-14* mutants initiate movement quiescence prematurely, and they display reduced levels of stress-induced sleep. Overexpression of *nlp-14* induces quiescence of movement and defecation.²⁹ We conducted a genetic screen to isolate suppressors of *nlp-14*-induced quiescence, similar to what was done for *fip-13*.^{37,38} Transgenic animals capable of overexpressing *nlp-14* were treated with the mutagen ethyl methanesulfonate (EMS), grown to the F2 generation, and induced to overexpress *nlp-14*. We fabricated gravity-based sorting devices from polylactic acid filament material, which we call “worm-ramps.” Worm-ramps have a lower loading chamber and an upper collection platform, separated by an 18° angled ramp (Figures 1A and S1). Animals undergoing movement quiescence remained in the loading chamber, whereas suppressor mutants navigated up the worm-ramp to the collection platform and were subsequently singled to a standard growth plate. The progeny of the suppressor strains were screened for their ability to suppress *nlp-14*-induced quiescence by counting body bends and using the WorMotel.³⁹ The strains *stj309*, *stj327*, *stj328*, and *stj330* displayed the strongest suppression (Figures 1B and 1C) and were thus subsequently analyzed by whole-genome sequencing (WGS) (Genewiz). Although the causative allele was determined for the *stj330* strain, the identities of the sleep-regulating genes in the other strains are still unknown.

stj330 animals harbored a G→A splice-variant mutation located 5' of exon 3 in the gene T10E10.3, a predicted GPCR⁴¹ (Figure 1D), which we named neuropeptide receptor-like-38 (*npr-38*). Using CRISPR, we constructed the mutant *npr-38(stj367)*, which contains an insertion of three stop codons

in exon 3. Additionally, we used CRISPR to insert an auxin-inducible degradation (AID) sequence at the 3' end to generate the strain *npr-38(stj452)* (Figure 1D).⁴² The AID-tagged strain allows for cell-specific degradation of the *npr-38* protein when the plant F box protein transport inhibitor response 1 (*tir1*) is expressed from cell-specific promoters.^{43,44} Last, we made a transcriptional reporter for *npr-38*, which was composed of the *npr-38* promoter fused to the *gfp* coding sequence. Transgenic animals expressing *npr-38p::gfp* showed expression in sensory and interneurons, including ADL, ASH, AIB, ALA, RIS, and DVA, and the pharyngeal neuron I6 (Figure 1E). This expression was consistent with the published transcriptomic data, which found *npr-38* expression additionally in RMG, I5, I2, and MC.⁴⁰ The transcriptomic data did not show expression in DVA; however, our reporter was expressed in this interneuron (Figure 1E).

npr-38 is required for stress-induced sleep and DTS

Considering that *npr-38* is required for the full induction of *nlp-14*-induced quiescence, we predicted that it would be required for stress-induced sleep⁸ and developmentally timed sleep (DTS).¹⁷ We measured movement quiescence during UV-induced stress-induced sleep¹⁵ in *npr-38(stj330)* and *npr-38(stj367)* animals. Both the total time spent in movement quiescence (i.e., sleep amount) and the duration of stress-induced sleep bouts were impaired in both strains (Figures 2A–2D), demonstrating that *npr-38* is required for the full expression of stress-induced sleep. *lin-3*/EGF signaling can activate the sleep neurons ALA and RIS.^{8,28} *lin-3* overexpression induces quiescence of movement.²⁷ We found that the *stj367* mutation only mildly suppressed this quiescence (Figure S2), suggesting that *npr-38* functions downstream and/or in parallel with *lin-3*.

Next, we measured DTS, which is controlled by distinct mechanisms.⁴⁵ We found that movement quiescence was reduced and the duration of DTS was shortened (Figures 2E–2G), demonstrating that *npr-38* is also required for DTS.

npr-38 is paralogous to the gene F59B2.13; we used CRISPR to create the mutant F59B2.13(*stj376*), which carries a 12-bp insertion of 3 stop codons in exon 4 (Figure S3A); however, these animals did not display stress-induced sleep defects. *npr-38(stj367)*; F59B2.13(*stj376*) double mutants displayed a reduction in movement quiescence similar to that in *npr-38* single mutants (Figures S3B–S3D). Thus, *npr-38* but not F59B2.13 regulates sleep.

Overexpression of *npr-38* disrupts sleep

Overexpression of GPCRs can induce gain-of-function phenotypes.^{46,47} We predicted that *npr-38* overexpression would heighten stress-induced sleep and DTS. We made transgenic, multi-copy overexpression lines. This included high-expressing lines (*npr-38(++)*; 50 ng/μL injection) and lower-expressing lines (*npr-38(+)*; 0.5 ng/μL injection). We were surprised to find that UV-induced sleep in *npr-38(++)* animals was not increased, but instead, these animals entered stress-induced sleep earlier than controls. Movement quiescence was induced almost immediately following stress exposure (Figure 3A), with movement quiescence being significantly higher in the first hour after UV exposure (Figure 3D). However, the total movement quiescence

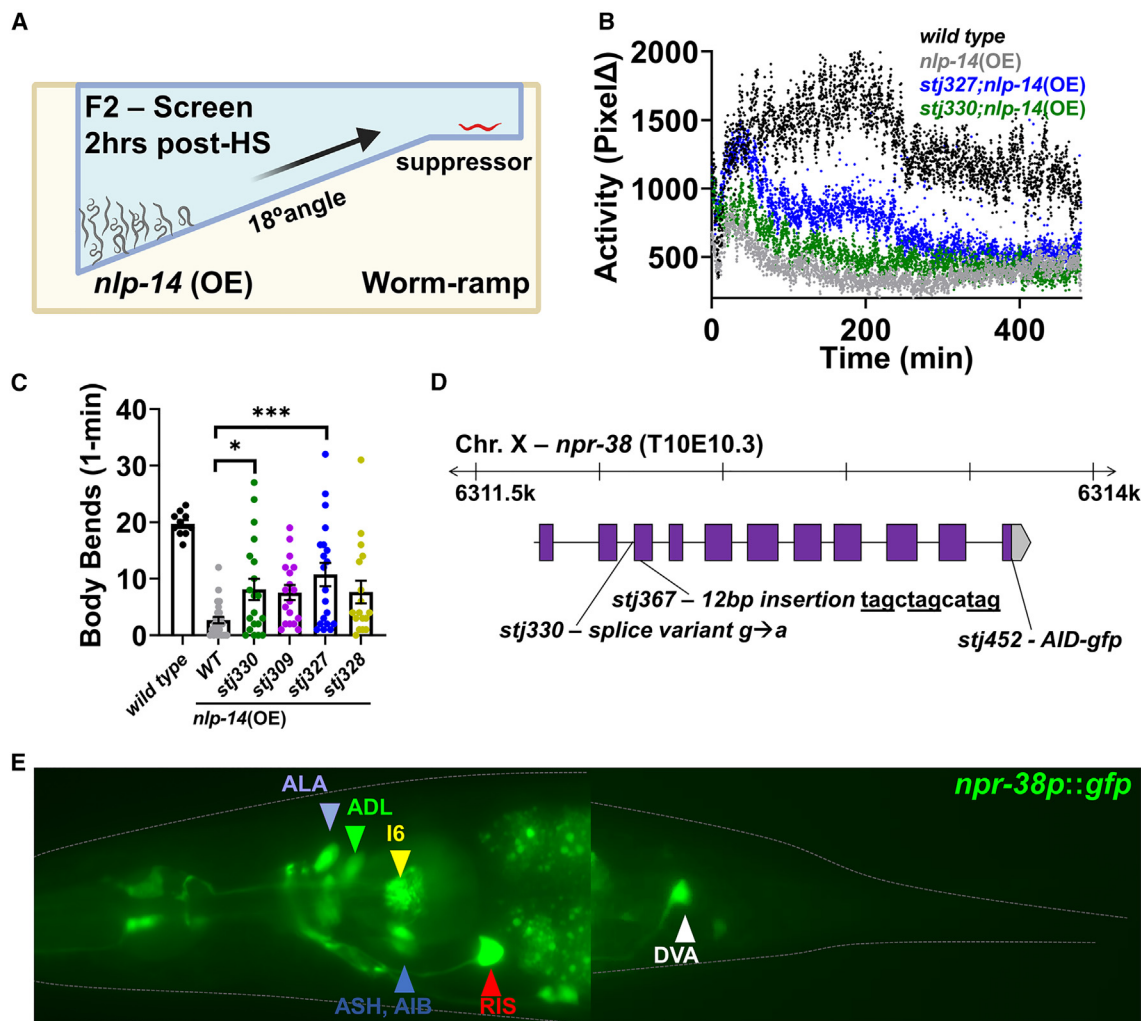


Figure 1. *npr-38* is required for *nlp-14*-induced sleep

(A) The *nlp-14* overexpression suppressor screen. Created with [BioRender.com](https://biorender.com).

(B) Activity after heat shock in wild-type, *nlp-14*(OE), *stj327;nlp-14*(OE), and *stj330;nlp-14*(OE) animals.

(C) Body bends in 1 min 2 h after heat shock in wild-type (n = 10), *nlp-14*(OE) (n = 26), *stj309;nlp-14*(OE) (n = 20), *stj327;nlp-14*(OE) (n = 18), *stj328;nlp-14*(OE) (n = 20), and *stj330;nlp-14*(OE) (n = 17) animals (*p < 0.05, ***p < 0.001, one-way ANOVA followed by Tukey's multiple comparisons test). Error bars represent SEM.

(D) Gene structure and alleles for *npr-38*.

(E) Expression of *npr-38p::gfp* is consistent with the *C. elegans* Neuronal Gene Expression Map & Network (CeNGEN),⁴⁰ except for the DVA. See also Figures S1 and S7.

during the 8-h recording was reduced, and the animals woke up prematurely (Figure 3C). Stress-induced sleep was initiated earlier in *npr-38*(+) animals but not to the same extent (Figures 3B and 3D), demonstrating a dosage effect. In *npr-38*(+)-L3 animals, movement quiescence was enhanced (Figure 3C). Thus, high overexpression can disrupt sleep, and lower overexpression can enhance it.

Animals were monitored during heat-induced sleep, which displays a unique temporal profile. Upon exposure to noxious heat (37°C–40°C), animals become immobile within minutes, a response that is ALA-independent.^{8,28} When animals encounter more favorable conditions, they remain quiescent, which is dependent on the ALA and RIS. This is followed by a period of activity and then a second wave of movement quiescence, which is ALA-dependent.⁸ We exposed *npr-38*(++) animals to

a 30-min heat shock at 37°C and measured quiescence using the WorMotel.³⁹ *npr-38*(++) animals displayed less quiescence in the 2-h period following the heat shock, showed a second wave of quiescence similar to controls, and overall displayed reduced total quiescence (Figures 3F and 3G). Thus, similar to UV-induced sleep, the animals woke prematurely following the stress.

We predicted that, similar to UV-induced sleep, they would immobilize more quickly upon heat exposure. We monitored the activity of wild-type, *npr-38*(++), and *npr-38*(stj367) animals every minute for 30 min in the presence of noxious heat (37°C). *npr-38*(++) animals became quiescent substantially earlier than controls, and *npr-38*(stj367) animals ceased movement later (Figure 3H). Thus, overexpression of *npr-38* causes early initiation of movement quiescence.

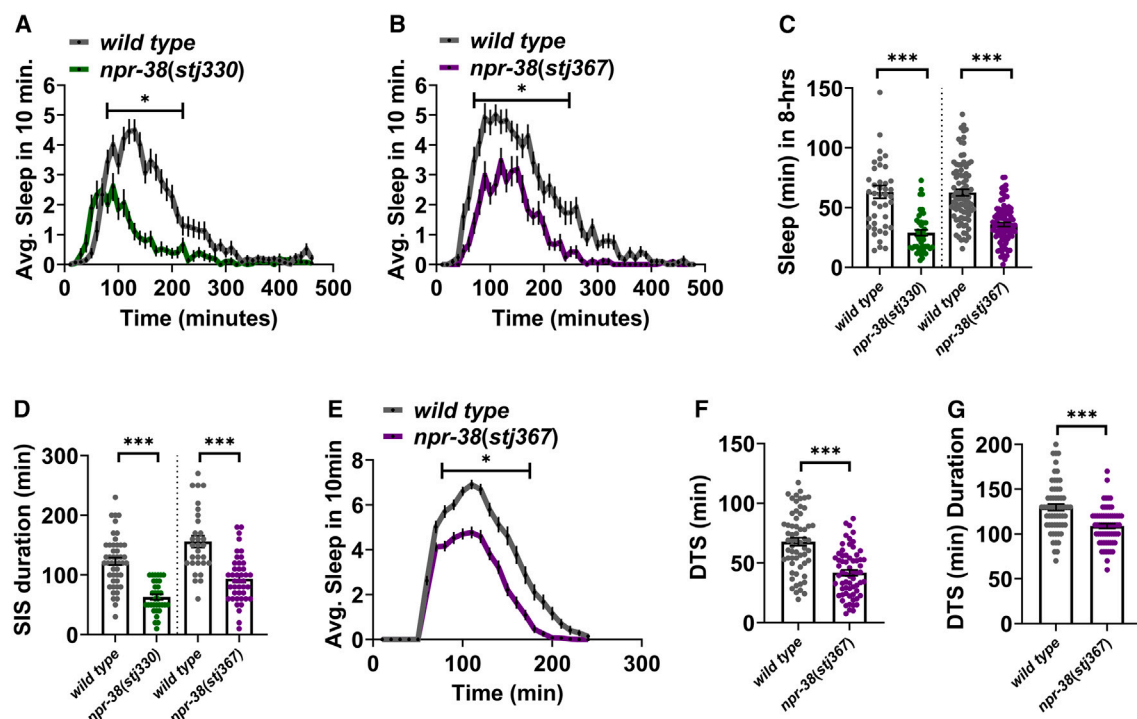


Figure 2. *npr-38* is required for sleep

(A) UV-induced sleep in wild-type ($n = 47$) and *npr-38(stj330)* ($n = 33$) animals ($^*p < 0.05$ at 120, 140, 160, and 250 min, $p < 0.01$ at 60–110, 130, 170, 180, 210, 220, 240, and 260).

(B) UV-induced sleep in wild-type ($n = 34$) and *npr-38(stj367)* ($n = 42$) animals ($^*p < 0.05$ at 60–140, 160–180, 210, 220, and 240–260 min).

(C) Total UV-induced sleep in wild-type ($n = 47$) and *npr-38(stj330)* ($n = 33$) and wild-type ($n = 34$) and *npr-38(stj367)* ($n = 42$) animals ($^{***}p < 0.001$).

(D) Duration of UV-induced sleep in wild-type ($n = 47$) and *npr-38(stj330)* ($n = 33$) and wild-type ($n = 34$) and *npr-38(stj367)* ($n = 42$) animals ($^{***}p < 0.001$).

(E) L4 developmentally timed sleep (DTS) in wild-type ($n = 60$) and *npr-38(stj367)* ($n = 64$) animals ($^*p < 0.001$ at 80–190 min).

(F) Total DTS in wild-type ($n = 60$) and *npr-38(stj367)* ($n = 64$) animals ($^{***}p < 0.001$).

(G) Duration of L4 DTS in wild-type ($n = 60$) and *npr-38(stj367)* ($n = 60$) animals ($^{***}p < 0.001$).

Statistical significance for (A), (B), and (E) was calculated using two-way ANOVA followed by Sidak's multiple comparisons test. Statistical significance for (C), (D), (F), and (G) was calculated using Student's *t* test. The dotted lines separate independent experiments. Error bars represent SEM. See also Figures S2, S3, and S7.

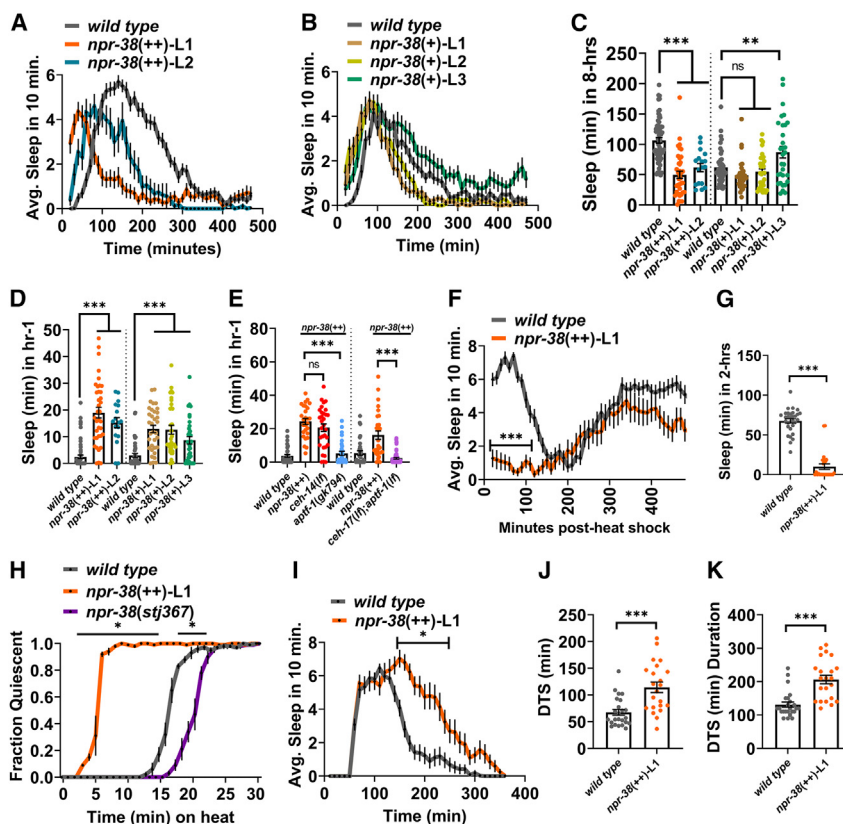
The RIS neuron is required for early movement quiescence of *npr-38(++)* animals

We reasoned that the early movement quiescence of *npr-38(++)* animals was caused by premature activation of sleep neurons. We measured movement quiescence in *ceh-14(ch3)* (ALA defective), *aptf-1(gk794)* (RIS defective), and *ceh-17(np1);aptf-1(gk794)* (ALA and RIS defective) animals who overexpressed *npr-38*. Disruption of the RIS but not the ALA prevented early movement quiescence (Figures 3E, S4A, and S4B); thus, the RIS is required for the early quiescence. However, because almost no movement quiescence was observed in *aptf-1;npr-38(++)* animals and overexpression is non-physiological, it is difficult to determine how *npr-38* connects with the RIS. *npr-38* is expressed in the RIS, and overexpression of *npr-38* specifically in the RIS disrupted movement quiescence (Figures S4H and S4I), which could indicate that *npr-38* inhibits the RIS, or these effects could be non-physiological.

Next, we measured movement quiescence during DTS in *npr-38(++)* animals. We found that total movement quiescence (Figures 3I and 3J) and the duration of DTS (Figure 3K) were enhanced. Thus, *npr-38* is required for and capable of increasing DTS.

npr-38 regulates sleep through the ADL sensory neurons

Next, we conducted rescue experiments based on the expression pattern of *npr-38* (Figure 4A).⁴⁰ First, we crossed a *npr-38(+)* line with *npr-38(stj367)* animals and measured stress-induced sleep. These *npr-38* genomic fragments restored movement quiescence to wild-type levels but caused stress-induced sleep to begin earlier than controls (Figures 4B and 4C). Next, we restored *npr-38* in *npr-38(stj367)* animals in the DVA using an enhancer element from the gene *twk-16*,⁴⁸ in the RIS using the *fpl-11* promoter,³² and in the ALA using the *ver-3* promoter.^{49,50} We were surprised to find that movement quiescence was not rescued by expression in any of these known sleep-regulating neurons (Figure 4B). Next, we restored *npr-38* in the ADL, AIB, ASH, and I6 neurons using the promoters from the genes *srh-220*, *npr-9*, *sra-6*, and *glr-6*.^{18,51–53} Rescue in the ADL strongly restored movement quiescence (Figures 4B and 4D), whereas rescue in the I6 mildly increased it (Figure 4B). We then expressed *npr-38* from the *ocr-2* promoter, which expresses in both ADL and ASH⁵⁴; this also restored movement quiescence (Figure 4B). Rescue in the ADL did not, however, restore movement quiescence during DTS (Figures S5A and S5B), but it did restore the animals' ability to respond



(I) DTS in wild-type (n = 24) and *npr-38*(++) (n = 22) animals (*p < 0.001 for 150–230, p < 0.05 for 240 and 260).
(J) Total L4 DTS in wild-type (n = 24) and *npr-38*(++) (n = 22) animals (**p < 0.001).

(K) Duration of L4 DTS in wild-type (n = 24) and *npr-38*(++) (n = 22) animals (**p < 0.001).

Statistical significance for (C)–(E) was calculated using one-way ANOVA followed by Tukey's multiple comparisons test. Statistical significance for (F), (H), and (I) was calculated using two-way ANOVA followed by Sidak's multiple comparisons test. Statistical significance for (G), (J), and (K) was calculated using Student's t test. Dotted line separates independent experiments and statistical comparisons. Error bars represent SEM. See also [Figures S4, S6, and S7](#).

appropriately to noxious heat ([Figure 4F](#)). Last, we overexpressed *npr-38* in the ADL neurons in wild-type animals; this modestly reduced stress-induced sleep ([Figure S4I](#)). These data suggest that *npr-38* functions in the ADL neurons to regulate stress-induced sleep.

To further test the requirement for *npr-38* in the ADL neurons, we expressed *tir-1* from the *srh-220* promoter in AID-tagged *npr-38(stj452)* animals to remove *npr-38* protein in the ADL neurons. Additionally, we made transgenic lines expressing *tir-1* in all somatic cells using the *eft-3* promoter. Transgenic *tir-1*-expressing *npr-38(stj452)* animals were transferred to plates supplemented with auxin or plates without auxin, and non-transgenic *npr-38(stj452)* controls were exposed to auxin for 4 h and subsequently monitored during UV-induced stress-induced sleep. Degradation of *npr-38* protein in all cells or in the ADL reduced movement quiescence ([Figures 4E](#) and [S5C](#)). However, we found that movement quiescence was reduced even in the absence of auxin. We speculate that this was caused by leakiness of the *tir-1* system.⁵⁶ The sleep defects were not as severe as *npr-38* mutants, possibly due to incomplete degradation. Expression of *tir-1* in the DVA neurons did not reduce movement quiescence ([Figure 4E](#)). Taken together

with our rescue experiments, these data support *npr-38* functioning in the ADL neurons.

npr-38 may inactivate the ADL neurons to promote sleep

Sensory neurons are less responsive during sleep;^{57,58} thus, we hypothesized that *npr-38* inhibits the ADL sensory neurons. We genetically ablated the ADL neurons by expressing the cell death-inducing gene *egl-1*⁵⁹ from the *srh-220* promoter. These animals displayed increased movement quiescence ([Figures 4G](#) and [4H](#)). Next, we ablated the ADL neurons in *npr-38(stj367)* mutant animals; this caused an increase in movement quiescence relative to *npr-38(stj367)* animals, with total levels lower than wild-type animals ([Figure 4H](#)). These data suggest that the ADL neurons promote arousal.

The TRPV-channels *osm-9* and *ocr-2* regulate stress-induced sleep

To further explore the role of the ADL neurons, we measured movement quiescence in mutants of the transient receptor potential cation (TRPV) channel-encoding genes *osm-9* and *ocr-2*, which are required in the ADL neurons for

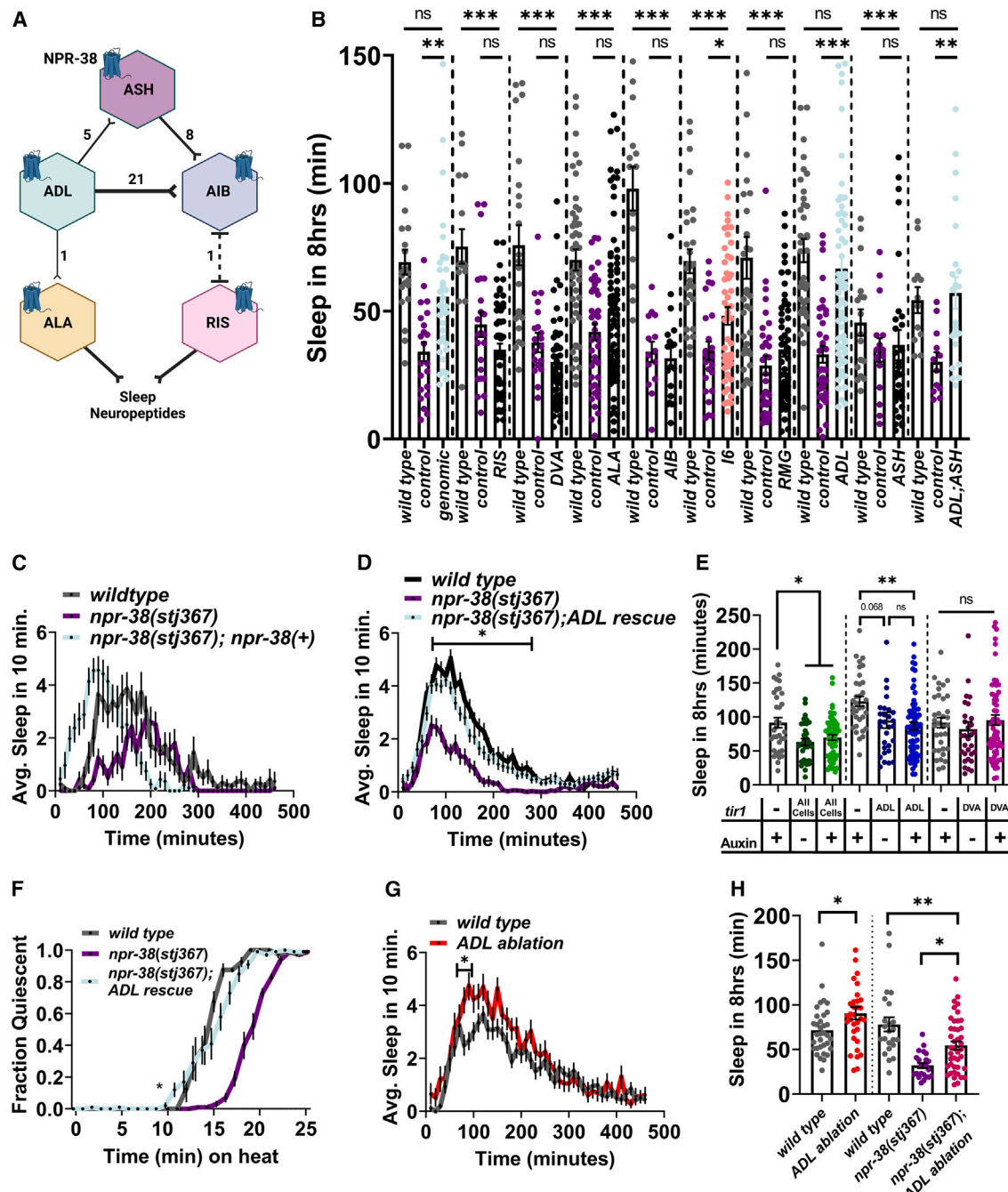


Figure 4. *npr-38* functions in the ADL neurons

(A) *npr-38* expression (solid lines = chemical synapses, dashed line = gap junction, and # = synapses).⁵⁵ Created with [BioRender.com](#).
 (B) Total UV-induced sleep in wild-type, *npr-38(stj367)* (control), and transgenic, rescued *npr-38(stj367)* animals (*p < 0.05, **p < 0.01, ***p < 0.001). Promoters: RIS, *fip-11*; DVA, *twk-16(cs1)::pes-10*; ALA, *ver-3*; AIB, *npr-9*; I6, *gtr-8*; RMG, *fip-21*; ADL, *srh-220*; ASH, *sra-6*; ADL + ASH, *ocr-2*. (Wild type, control, rescue): genomic rescue (n = 21, 22, 36), RIS (n = 15, 23, 57), DVA (n = 22, 20, 46), ALA (n = 46, 43, 80), AIB (n = 14, 14, 19), I6 (n = 28, 25, 51), RMG (n = 34, 32, 55), ADL (n = 26, 37, 70), ASH (n = 17, 16, 36), ADL + ASH (n = 12, 12, 23).
 (C) UV-induced sleep in wild-type (n = 21), *npr-38(stj367)* (n = 22), and *npr-38(stj367);npr-38(+)* animals (n = 36).
 (D) UV-induced sleep in wild-type (n = 26), *npr-38(stj367)* (n = 37), and *npr-38(stj367);srh-220p::npr-38* animals (n = 70) (*p < 0.05 at 40, 190, 220, and 240, p < 0.01 at 60–180 and 200).
 (E) Total UV-induced sleep in *npr-38(stj452)* animals on auxin (n = 33), and *npr-38(stj452);eft-3p::tit1* animals, on and off auxin (n = 57 and 34). And, *npr-38(stj452)* animals on auxin (n = 34), and *npr-38(stj452);srh-220p::tit1* animals on and off auxin (n = 65 and 31). And, in *npr-38(stj452)* animals on auxin (n = 31), and *npr-38(stj452);twk-16(cs1)::tit1* animals on and off auxin (n = 64 and 31) (*p < 0.05, **p < 0.01).

(legend continued on next page)

thermosensation.¹⁸ *osm-9* regulates heat avoidance by acting in the ADL neurons, and *ocr-2* regulates UV avoidance through the ASH neurons, which also express *npr-38*.^{60,61} Both neurons signal through the RMG circuit, which regulates arousal via the neuropeptide Y receptor *npr-1*,⁶² and also expresses *npr-38*. *npr-1* mutants are defective in UV-induced sleep, which is suppressed by mutations in *osm-9*.¹⁰ We found that *osm-9* mutants were defective in total levels of movement quiescence during UV-induced sleep (Figures 5A and 5C). *ocr-2* mutants also displayed reduced movement quiescence (Figures 5B and 5C); additionally, they showed an early movement quiescence phenotype, similar to animals that overexpress *npr-38* (Figures 5B and 5D). In the presence of noxious heat, *osm-9* mutants entered a quiescent state later than wild-type controls, whereas *ocr-2* mutants initiated movement quiescence earlier (Figure 5E). In summary, *osm-9* mutants behaved similarly to *npr-38* mutants, whereas *ocr-2* mutants resembled *npr-38* overexpression animals.

npr-38* interacts genetically with *nlp-14* and *nlp-8

The ADL neurons are glutamatergic⁶³ and express neuropeptide-encoding genes, including *nlp-14*, *nlp-8*, and *flp-21*.⁴⁰ *nlp-8*³⁰ and *nlp-14*²⁹ regulate sleep, whereas *flp-21* regulates avoidance.⁶⁴ We hypothesized that *npr-38* is a receptor for *nlp-14*, considering *npr-38* is required for the full induction of *nlp-14*-induced sleep (Figure 1). If *npr-38* is an *nlp-14* receptor, then loss of function of *nlp-14* should disrupt the phenotypes induced by *npr-38* overexpression. Additionally, we tested for the requirement of *nlp-8*, *nlp-15*, and *flp-21* for the *npr-38* overexpression phenotypes. Mutations in *nlp-8* reduced the early movement quiescence and the total levels overall (Figures S4C and S4D), whereas *nlp-14*, *nlp-15*, and *flp-21* did not (Figure S4D). These data argue against *npr-38* being an *nlp-14* receptor and instead implicate *nlp-8*. To test this further, we measured movement quiescence in wild-type and *npr-38(stj367)* animals capable of overexpressing *nlp-8* from the inducible heat shock promoter (Figures S4E–S4G). As previously demonstrated,³⁰ overexpression of *nlp-8* inhibits movement in wild-type animals, and this was not suppressed in the *npr-38(stj367)* mutant background. These data suggest that *nlp-8* peptides are not ligands for *npr-38* and instead that *nlp-8* function downstream. Future work will be needed to identify the ligands for *npr-38*.

Considering *npr-38* was identified in an *nlp-14* overexpression suppressor screen, we sought to further explore the interactions between these two genes. We constructed an *nlp-14;npr-38* double mutant. Loss of both genes caused a substantial reduction in stress-induced sleep and resulted in a sleep profile different from both the *npr-38* and *nlp-14* single mutants (Figures S6A–S6C). Double mutants displayed movement

quiescence similar to the *npr-38* single mutants but significantly lower than *nlp-14* mutants (Figure S6C). Furthermore, the early movement quiescence phenotype of *nlp-14* mutants²⁹ was attenuated in *npr-38;nlp-14* double mutants (Figures S6A and S6D). These data suggest a complex interaction between *npr-38* and *nlp-14* but indicate that *nlp-14* does not encode peptides for the *npr-38* receptor.

Optogenetic activation of the ADL neurons promotes arousal

Our data support a model in which *npr-38* functions to promote sleep by inhibiting the ADL neurons. Thus, we predicted that optogenetic activation of the ADL neurons would promote movement and possibly disrupt sleep. We expressed ChannelRhodopsin-2 (ChR2) from the *srh-220* promoter and exposed animals to blue light 15 min before UV stress and 15, 30, 45, 60, 75, 90, and 120 min following stress (Figure 6A). Transgenic control animals that were exposed to blue light but not grown on all-trans-retinol (ATR) showed a progressive decrease in body bending throughout the experiment. Optogenetic activation of the ADLs increased body bending at each time-point tested, even before UV stress was applied. After UV exposure, the arousal effects of ADL activation were more prominent at the earlier time points (15–45 min), which coincides with the time frame before movement quiescence. As movement quiescence was initiated, animals were more resistant to arousal by blue light. Additionally, optogenetic activation of the ADL neurons for 1 min immediately after UV stress and every 15 min for 2 h only modestly reduced total movement quiescence (Figures 6B and 6C). These data suggest that ADL activation is important during the avoidance phase and may function to delay sleep entry; however, ADL activation alone is not sufficient to overcome the action of the sleep circuitry.

***nlp-50* encodes wake-promoting peptides expressed in the ADLs**

Which neurotransmitters are released from the ADL neurons to stimulate arousal? Based on transcriptomic data, the neuropeptide-encoding gene *nlp-50* is one of the most highly enriched signaling molecules in the ADL neurons.⁴⁰ We used CRISPR to construct the strain *nlp-50(stj553)*, which possesses a 267 bp deletion and a 4 bp insertion, which results in a frameshift (Figure 6D). *nlp-50(stj553)* animals displayed less movement quiescence than wild-type controls during stress-induced sleep (Figures 6E and 6G), suggesting that *nlp-50* encodes sleep-promoting neuropeptides. Thus, we predicted that overexpression would lead to enhanced sleep. We made extrachromosomal transgenic lines that express additional copies of the *nlp-50* gene. Stress-induced sleep was significantly impaired in these transgenic strains (Figures 6H and 6I), demonstrating that

(F) Fraction quiescent on heat in wild-type, *npr-38(stj367)*, and *npr-38(stj367);srh-220p::npr-38* animals ($n = 20$ per 5 trials, $^*p < 0.01$ for time 11–20 comparing *npr-38(stj367)* with ADL rescue).

(G) UV-induced sleep in wild-type ($n = 34$) and *srh-220p::egl-1* ($n = 33$) animals.

(H) Total UV-induced sleep in wild-type ($n = 34$) and *srh-220p::egl-1* ($n = 33$), and wild-type ($n = 23$), *npr-38(stj367)* ($n = 23$), and *npr-38(stj367);srh-220p::egl-1* animals ($n = 42$) ($^*p < 0.05$, $^{**p} < 0.01$).

Statistical significance for (B), (E), and (H) was calculated using one-way ANOVA followed by Tukey's multiple comparisons test. Statistical significance for (D), (F), and (G) was calculated using two-way ANOVA followed by Sidak's multiple comparisons test. Dashed lines separate independent experiments and statistical comparisons. Error bars represent SEM. See also Figures S5–S7.

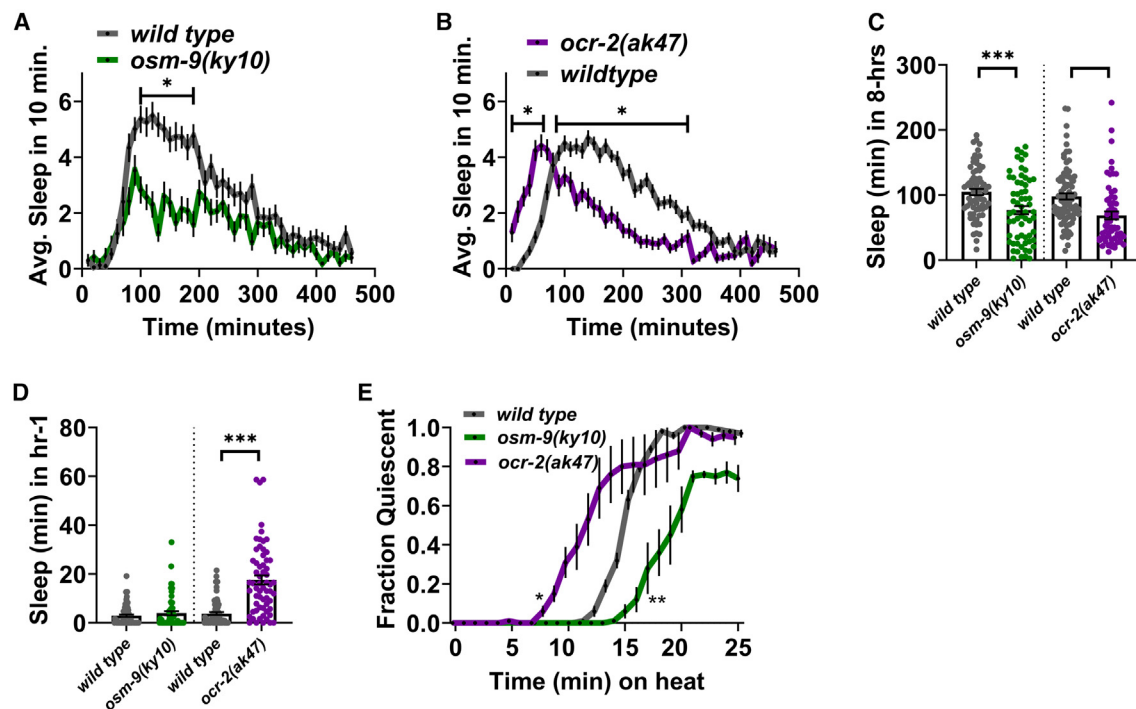


Figure 5. *osm-9* and *ocr-2* regulate stress-induced sleep

(A) UV-induced sleep in wild-type ($n = 35$) and *osm-9(ky10)* animals ($n = 29$) (${}^*p < 0.05$ at 90 min, $p < 0.001$ for 100–190).
 (B) UV-induced sleep in wild-type ($n = 84$) and *ocr-2(ak47)* animals ($n = 62$) (${}^*p < 0.05$ at 10, 270, and 320 min, $p < 0.01$ at 70, 130, 260, and 290, $p < 0.001$ at 20–60, 120, 140–250, and 280 min).
 (C) Total quiescence during UV-induced sleep in wild-type ($n = 71$) and *osm-9(ky10)* ($n = 63$), and wild-type ($n = 84$) and *ocr-2(ak47)* animals ($n = 62$) (${}^{***}p < 0.001$).
 (D) Quiescence in 1 h of UV-induced sleep in wild-type ($n = 71$) and *osm-9(ky10)* ($n = 63$), and wild-type ($n = 84$) and *ocr-2(ak47)* animals ($n = 62$) (${}^{***}p < 0.001$).
 (E) Fraction of animals quiescent during heat exposure (37°C) in wild-type, *osm-9(ky10)*, and *ocr-2(ak47)* animals ($n = 20$ per 5 trials, ${}^*p < 0.01$ for 16–19 min [wild type to *osm-9(ky10)*], and ${}^{**}p < 0.01$ for 11–17 [wild type to *ocr-2(ak47)*]).

Statistical significance for (A), (B), and (E) was calculated using two-way ANOVA followed by Sidak's multiple comparisons test. Statistical significance for (C) and (D) was calculated using Student's *t* test. Dashed lines separate independent experiments and statistical comparisons. Error bars represent SEM. See also Figure S7.

nlp-50 is both required for sleep and can disrupt sleep when overexpressed. *nlp-50* is expressed broadly in the nervous system⁴⁰; one possibility is that *nlp-50* promotes arousal when released from one location and sleep from another. To better understand the role *nlp-50* plays, we rescued *nlp-50* in the ADL neurons in *nlp-50(stj553)* animals. Not only did this not rescue movement quiescence, it further reduced it (Figures 6F and 6G), suggesting that *nlp-50* promotes arousal in the ADL neurons. Identifying a receptor for *nlp-50* will be an important next step in understanding these mechanisms.

***npr-38* promotes arousal during wakefulness**

npr-38 mutants are defective in their ability to respond to stress and the recovery sleep that occurs shortly after. Additionally, we noticed that *npr-38* mutants display a reduction in movement during times of normal wakefulness, suggesting that *npr-38* plays a role in promoting general arousal. Activity levels and body bending were lower in *npr-38* mutants compared with wild-type controls (Figures 7A–7C). Normal movement activity was restored by crossing *npr-38(stj367)* mutants with one of the lower-expressing *npr-38(+)* lines (Figure 7C). Expression of *npr-38* in the RIS or DVA interneurons in *npr-38(stj367)* animals restored body bends to wild-type

levels; expression in ADL, ALA, or I6 did not (Figure 7C). Our *npr-38* reporter shows expression in the DVA (Figure 1E); however, transcriptomic analyses did not detect *npr-38* in this neuron.⁴⁰ Thus, the RIS may represent the physiological site of action. Additionally, *nlp-14;npr-38* double mutants showed activity levels comparable to *nlp-14* single mutants (Figure S6E), further demonstrating a complex interaction between these two genes. Paradoxically, *npr-38(++)* animals were also less active (Figure 7B); however, qualitatively, these animals were more sensitive to mechanical stimulation. Reduced responsiveness to stimuli is a hallmark characteristic of sleep.⁶⁵ To determine if *npr-38* was required for sensory responsiveness, we measured the reaction to blue light, an aversive stimulus.¹⁴ Unstressed *npr-38(stj367)* animals were less responsive than wild-type controls (Figure 7D), whereas *npr-38* overexpressing animals responded similarly to wild type (Figure 7D). Thus, *npr-38* mutant animals are less responsive to blue light and may fail to avoid it.

To observe avoidance over a longer timescale, we measured movement in response to blue light during 5-min exposures. We compared the activity of *npr-38(stj367)* animals with both wild-type controls and paralyzed *unc-31* mutants who can be stimulated to move by sustained blue light.¹⁴

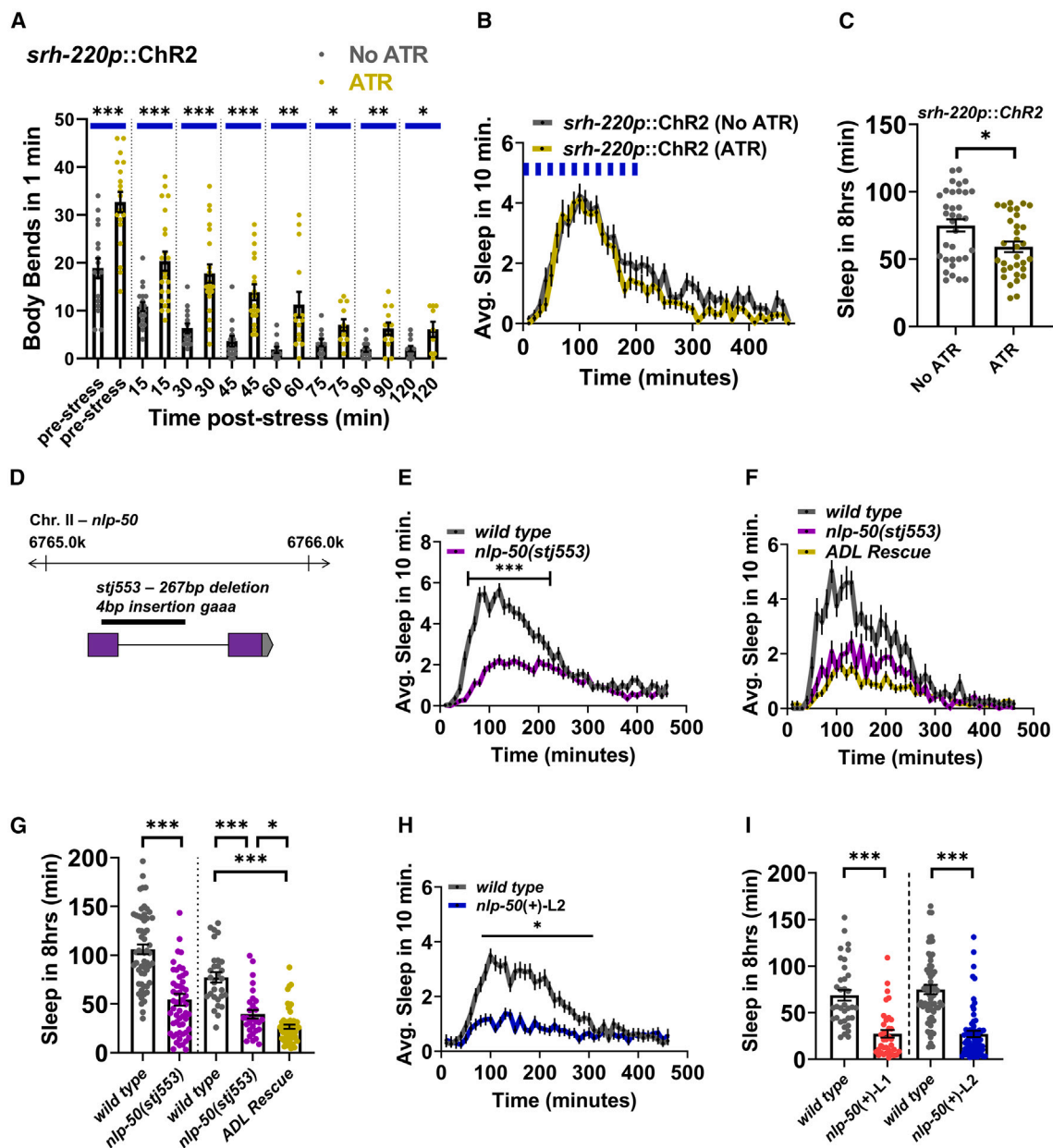


Figure 6. The ADL neurons promote arousal

(A) Body bends under blue light by *srh-220p::ChR2* animals on and off all-trans-retinol (ATR); before UV-shock (pre-stress) (n = 17 [no ATR] and n = 19 [ATR]), and at 15 (n = 18 [no ATR] and n = 22 [ATR]), 30 (n = 14 [no ATR] and n = 21 [ATR]), 45 (n = 14 [no ATR] and n = 19 [ATR]), 60 (n = 12 [no ATR] and n = 14 [ATR]), 75 (n = 11 [no ATR] and n = 11 [ATR]), 90 (n = 12 [no ATR] and n = 12 [ATR]), and 120 min post stress (n = 12 [no ATR] and n = 9 [ATR]) (*p < 0.05, **p < 0.01, ***p < 0.001).

(B) UV-induced sleep in *srh-220p::ChR2* animals on (n = 34) and off ATR (n = 32).

(C) Total UV-induced sleep in *srh-220p::ChR2* animals on (n = 34) and off ATR (n = 32) (*p < 0.05). For (B) and (C), blue light (blue bars) occurred every 15 min for 2 h.

(D) Gene structure and allele for *nlp-50*.

(E) UV-induced sleep in wild-type (n = 56) and *nlp-50(stj553)* animals (n = 56) (**p < 0.001 at 50–190).

(F) UV-induced sleep in wild-type (n = 29), *nlp-50(stj553)* (n = 29), and *nlp-50(stj553);srh-220p::nlp-50* animals (n = 56) (**p < 0.001).

(G) Total UV-induced sleep in wild-type (n = 56) and *nlp-50(stj553)* animals (n = 56) (**p < 0.001) and wild-type (n = 29), *nlp-50(stj553)* (n = 29), and *nlp-50(stj553);srh-220p::nlp-50* animals (n = 56).

(H) UV-induced sleep in wild-type (n = 62) and *nlp-50(+)-L2* animals (n = 66, *p < 0.05 at 80–230 min).

(I) Total UV-induced sleep in wild-type (n = 34 and 62) and *nlp-50(+)* animals (n = 35 and 66, ***p < 0.001).

Statistical significance for (A), (C), and (G) (left) was calculated using Student's t test, for (G) (right) by one-way ANOVA followed by Tukey's multiple comparisons test, and for (E) and (H) by two-way ANOVA followed by Sidak's multiple comparisons test. The dashed lines separate statistical comparisons. Error bars represent SEM. See also Figures S5–S7.

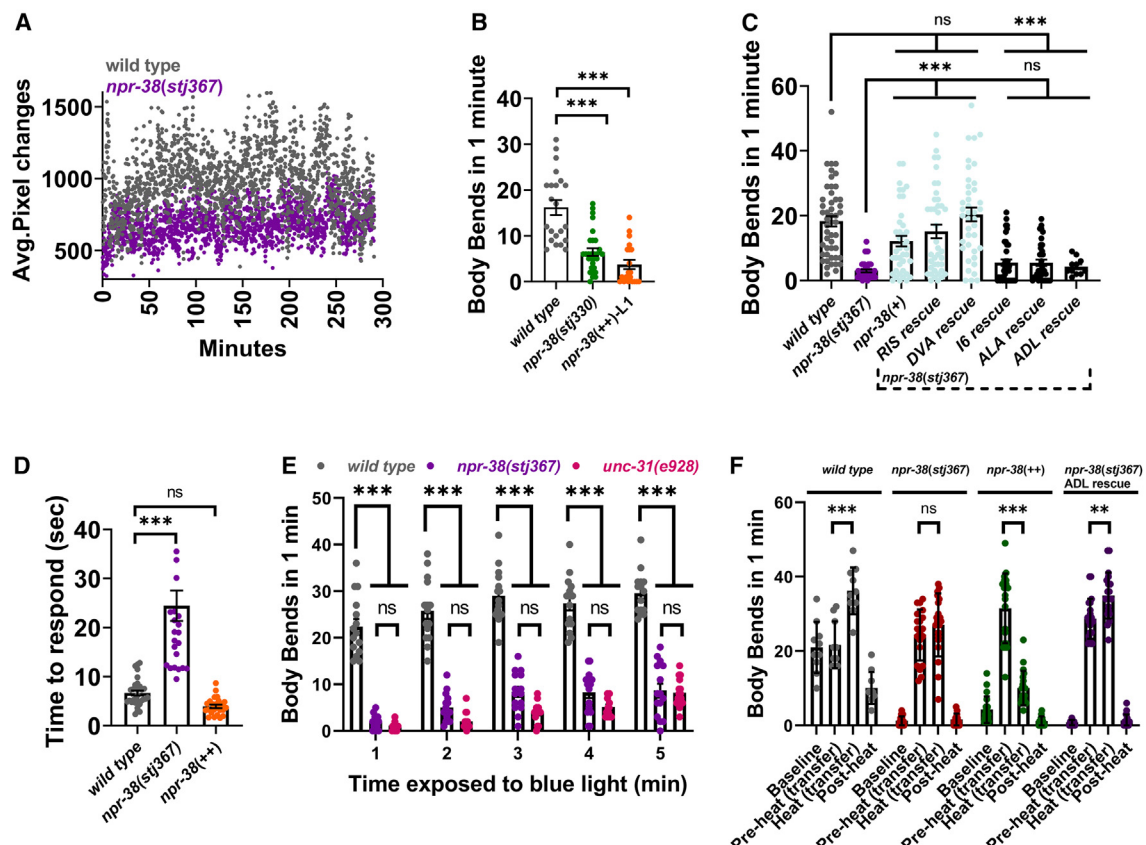


Figure 7. *npr-38* regulates arousal

(A) Pixel changes in 10 s in wild-type ($n = 6$) and *npr-38(stj367)* ($n = 18$) adults.

(B) Body bends by wild-type ($n = 50$), *npr-38(stj330)* ($n = 29$), and *npr-38(++)* ($n = 27$) animals ($***p < 0.001$).

(C) Body bends by wild-type ($n = 22$), *npr-38(stj367)* ($n = 41$), and *npr-38(stj367)* animals expressing genomic fragments of *npr-38* ($n = 40$), or *npr-38* in: RIS ($n = 40$), DVA ($n = 40$), I6 ($n = 39$), ALA ($n = 36$), ADL ($n = 11$).

(D) Response time in wild-type, *npr-38(stj367)*, and *npr-38(++)* animals ($n = 20$, $***p < 0.001$).

(E) Body bends in wild-type, *npr-38(stj367)*, and *unc-31(e928)* animals ($n = 15$, $***p < 0.001$).

(F) Body bends in wild-type, *npr-38(stj367)*, and *npr-38(stj367);srf-220p::npr-38* animals ($n = 20$, $**p < 0.01$, $***p < 0.001$). One-way ANOVA followed by Tukey's multiple comparisons test was used for all analyses. Error bars represent SEM. See also Figures S6 and S7.

npr-38 and *unc-31* mutants behaved similarly, in that they increased locomotion in the presence of blue light over time but moved significantly less than wild-type animals (Figure 7E). These data suggest that *npr-38* mutants fail to avoid blue light.

Next, we assessed the ability of *npr-38* mutants to respond to mechanical stimulation and heat. Baseline body bends were quantified, and then animals were transferred to room-temperature plates and then to warmed plates (35°C), body bends were quantified following each transfer. The plates were allowed to cool for 30 min to room temperature, at which point body bends were quantified again. Wild-type animals increased their movement in response to heat (Figure 7F); however, *npr-38* animals only increased locomotion following the initial transfer but not in the presence of heat. Their ability to respond to heat was restored by ADL rescue (Figure 7F). This demonstrates that *npr-38* animals respond robustly to mechanical stimuli, and that they are defective in their ability to respond to heat. *npr-38*-overexpressing animals also increased locomotion following the initial transfer, but when moved to a heated

plate, their movement slowed, indicative of early quiescence (Figure 7F).

As a whole, our data suggest that *npr-38* promotes arousal outside of sleep through the RIS and possibly the DVA neurons and regulates avoidance by acting through the ADL neurons. Thus, *npr-38* regulates multiple aspects of the stress response: avoidance, sleep, and arousal.

DISCUSSION

We identified the GPCR-encoding gene *npr-38*, which is required for sleep in *C. elegans*. *npr-38* mutants display a reduction in movement quiescence during developmentally-timed sleep and stress-induced sleep, the latter of which was the focus of this study. *npr-38* is expressed in the ALA⁸ and RIS³⁶ sleep neurons, the wake-promoting DVA neuron,³⁴ and the RMG circuitry that controls arousal.¹⁰ *npr-38* is required in the ADL neurons during stress-induced sleep, which are connected to the ALA and RIS. ADL chemically synapses on the ALA and the AIB, the latter having gap junctions on the RIS.⁵⁵ Thus, the

ADL sensory neurons are connected to the sleep circuitry and represent a new sleep neuron pair. Although the ALA and RIS increase their activity during sleep,^{28,36,66,67} we propose that the ADL neurons are less active. Considering *npr-38* is expressed in all four cells of this circuitry (ADL, ALA, AIB, and RIS) (Figure 4A), as well as the wake-promoting DVA neuron, one possibility is that *npr-38* coordinates the transition between avoidance and sleep. We propose that during wakefulness, *npr-38* promotes arousal and avoidance but then generally suppresses arousal during sleep. This is supported by the fact that overexpression of *npr-38* causes animals to prematurely stop avoidance and enter a sleep state earlier than wild-type animals. This early movement quiescence requires the RIS interneuron and some known sleep peptides. Additionally, *npr-38* is required in the RIS and DVA neurons for arousal outside of sleep. Taken together, we propose a model in which the ADL neurons, via the release of *nlp-50* peptides, enhance the avoidance response before sleep initiation. At the same time, *npr-38* may inhibit the RIS and/or activate the DVA to promote arousal. Once clear of stress, we speculate that unknown sleep peptides bind to *npr-38* inactivating the ADL and DVA neurons to suppress arousal. At this point, *lin-3* and *nlp-50* are released from other locations to promote sleep and suppress arousal (Figure S7).

ADL sensory neurons detect environmental stimuli, including temperature,^{18,68} pheromones,⁶⁹ and chemicals, such as DEET,⁷⁰ heavy metals,⁷¹ and octanol.⁷² Additionally, they coordinate preferences for bacterial foods,⁵¹ and cold tolerance.⁷³ Our work has identified additional roles for the ADL neurons as sleep-regulators. The diversity in function is reflected by an underlying complexity of signaling molecules expressed in the ADL neurons. They are glutamatergic; glutamate promotes arousal by inhibiting sleep circuitry in *Drosophila*⁷⁴ and mammals.⁷⁵ Additionally, glutamate is wake-promoting during developmentally-timed sleep in *C. elegans*,^{24,76} making it a potential signal during the arousal of stress-induced sleep. The ADL neurons also express many neuropeptide-encoding genes, which include *flp-4*, *fip-5*, *fip-16*, *fip-25*, *nlp-8*, *nlp-14*, *nlp-50*, *nlp-61*, *nlp-63*, and others.^{40,51} Of these, *nlp-8* and *nlp-14* are known to regulate stress-induced sleep and are expressed in the ALA neuron^{29,30}; however, the functions of the other peptides have not been extensively explored. Our data suggest that *npr-38* functions upstream of these signals. One possibility is that during avoidance, the ADL neurons remain active due to sensory stimulation, which causes the release of wake-promoting factors such as *nlp-50* and glutamate. Following escape, *npr-38* can then function to inhibit the ADL neurons and promote movement quiescence. At this point, it is unclear what role the ADL-expressed sleep-promoting factors play, but positive feedback may aid in ADL neuron inhibition.

How the *nlp-14*/orcokinin peptides interact with the *npr-38* pathway is likely complex. Enhancing *npr-38* signaling by overexpression causes avoidance to terminate and movement quiescence to initiate early. A similar phenotype occurs in the context of *nlp-14* loss of function. However, *npr-38;nlp-14* double mutants initiate movement quiescence at the correct time but display very low levels of quiescence. Based on these observations, one possibility is that *nlp-14* signaling antagonizes *npr-38* to promote arousal during the avoidance phase; however, both pathways likely function in parallel to promote sleep at later

stages. Positively identifying the *nlp-14* and *nlp-50* receptor(s), the *npr-38* ligand(s), and additional sleep-regulating neurotransmitters of the ADL neurons will be essential steps in further understanding these mechanisms.

Despite lacking a clear picture of the signaling mechanisms of the ADL neurons, it is clear that they are involved in regulating arousal. The TRPV channel encoded by *osm-9*, which functions in the ADL, is required for oxygen avoidance.⁷⁷ Ambient oxygen disrupts stress-induced sleep, which is coordinated by *npr-1*. *npr-1* mutants display heightened arousal in hyperoxic conditions, which is dependent on *osm-9*.¹⁰ This indicates that the ADL promotes oxygen avoidance; however, our experiments, performed under normoxic conditions, suggest a more complicated role. We find that *osm-9* and *npr-38* mutants display increased arousal during stress-induced sleep, considering their avoidance occurs for a longer period than wild-type animals (Figure 5E), and they display reduced levels of total movement quiescence (Figures 5A and 5C). Restoring *npr-38* specifically in the ADL rescues these phenotypes. Additionally, *ocr-2* mutants more closely resemble *npr-38* overexpressing animals in that they initiate movement quiescence early and have overall reduced levels of it (Figures 5B, 5C, and 5E). *ocr-2* also functions in the ADL neurons.²³ The ADL neurons, thus, regulate both avoidance and sleep, how this is coordinated is unclear. Making this more complicated is the possibility that the ADL neurons may respond differently to distinct stimuli (i.e., O₂, heat, and UV). How ADL activity is connected with sleep neuron activation is still unclear.

Interestingly, *npr-38* is expressed in the sleep circuitry and acts antagonistically to the ADL neurons (Figure 4A). Restoration of *npr-38* in the ALA or RIS does not rescue the sleep defects of *npr-38* mutants. The cessation of movement during sleep is precisely correlated with RIS activation, and the resumption of locomotion immediately follows RIS inactivation.^{28,36,67} ALA activation precedes movement quiescence and is required for the full activation of the RIS during stress-induced sleep.²⁸ Our data indicate that *npr-38* inhibits RIS activity, considering that select expression of *npr-38* in the RIS in wild-type animals strongly reduces movement quiescence (Figures S4H and S4I). Also, expression of *npr-38* in the RIS in *npr-38* mutants restores the activity normally observed in awake animals, which is impaired in *npr-38* mutants (Figure 7C). Expression specifically in the DVA using a well-defined enhancer element⁴⁸ also restores this activity (Figure 7C). Arousal from stress-induced sleep is mediated downstream of GPCR signaling by cyclic adenosine monophosphate (cAMP); optogenetic activation of cAMP in the DVA disrupts movement quiescence.³⁴ We speculate that *npr-38* uniquely modulates second messengers in different cells to decrease the activity of some, such as the RIS and ADL, and increase the activity of others, such as the DVA, establishing a balance between sleep-wake circuits.

Sleep state transitions must be precisely coordinated so that animals can wake up rapidly from sleep and, in the case of stress-induced sleep in *C. elegans* escape before falling asleep. Sleep-wake transition states in mammals are controlled by mutual inhibitory interactions between arousal and sleep circuits,⁷⁸ and a similar circuit architecture may underlie sleep in *C. elegans*.⁷⁹ Our work demonstrates that within the compact 302-celled nervous system of *C. elegans*, *npr-38* may sit at the interface of this circuitry.

STAR★METHODS

Detailed methods are provided in the online version of this paper and include the following:

- **KEY RESOURCES TABLE**
- **RESOURCE AVAILABILITY**
 - Lead contact
 - Materials availability
 - Data and code availability
- **EXPERIMENTAL MODEL AND SUBJECT DETAILS**
- **METHOD DETAILS**
 - Genetic screen
 - Molecular biology and transgenesis
 - Construction of mutants
 - WorMotel behavioral assays
 - Avoidance and body bending analyses
 - Optogenetic experiments
 - Quiescence during heat exposure
 - Microscopy
- **QUANTIFICATION AND STATISTICAL ANALYSES**

SUPPLEMENTAL INFORMATION

Supplemental information can be found online at <https://doi.org/10.1016/j.cub.2023.06.042>.

ACKNOWLEDGMENTS

Some strains were provided by the CGC, which is funded by the NIH Office of Research Infrastructure Programs (P40 OD010440). We thank David Raizen, Alex Rohacek, and Paul Sternberg for sharing reagents and strain constructions. We would also like to thank the SJU Summer Scholars Program and the John P. McNulty Fellows Program. M.D.N. was supported by the National Science Foundation grants IOS-1845020 and DBI-MRI-1919847.

AUTHOR CONTRIBUTIONS

M.D.N. designed the experiments and wrote the manuscript. M.D.N., E.L., T.M., C.E.C., M.H., and J.F. conducted the experiments and analyzed and interpreted the results.

DECLARATION OF INTERESTS

The authors declare no competing interests.

Received: December 18, 2022

Revised: May 19, 2023

Accepted: June 14, 2023

Published: July 6, 2023

REFERENCES

1. Keene, A.C., and Duboue, E.R. (2018). The origins and evolution of sleep. *J. Exp. Biol.* **221**, jeb159533.
2. Walker, J.M., and Berger, R.J. (1980). Sleep as an adaptation for energy conservation functionally related to hibernation and shallow torpor. *Prog. Brain Res.* **53**, 255–278.
3. Van Cauter, E., Spiegel, K., Tasali, E., and Leproult, R. (2008). Metabolic consequences of sleep and sleep loss. *Sleep Med.* **9**, S23–S28.
4. Frank, M.G., and Benington, J.H. (2006). The role of sleep in memory consolidation and brain plasticity: dream or reality? *Neuroscientist* **12**, 477–488.
5. Imeri, L., and Opp, M.R. (2009). How (and why) the immune system makes us sleep. *Nat. Rev. Neurosci.* **10**, 199–210.
6. Anafi, R.C., Kayser, M.S., and Raizen, D.M. (2019). Exploring phylogeny to find the function of sleep. *Nat. Rev. Neurosci.* **20**, 109–116.
7. Dubowy, C., and Sehgal, A. (2017). Circadian rhythms and sleep in *Drosophila melanogaster*. *Genetics* **205**, 1373–1397.
8. Hill, A.J., Mansfield, R., Lopez, J.M., Raizen, D.M., and Van Buskirk, C. (2014). Cellular stress induces a protective sleep-like state in *C. elegans*. *Curr. Biol.* **24**, 2399–2405.
9. Lenz, O., Xiong, J., Nelson, M.D., Raizen, D.M., and Williams, J.A. (2015). Fmr1amide signaling promotes stress-induced sleep in *Drosophila*. *Brain Behav. Immun.* **47**, 141–148.
10. Soto, R., Goetting, D.L., and Van Buskirk, C. (2019). NPR-1 modulates plasticity in *C. elegans* stress-induced sleep. *iScience* **19**, 1037–1047.
11. Chiu, I.M., Heesters, B.A., Ghasemlou, N., Von Hehn, C.A., Zhao, F., Tran, J., Wainger, B., Strominger, A., Muralidharan, S., Horswill, A.R., et al. (2013). Bacteria activate sensory neurons that modulate pain and inflammation. *Nature* **501**, 52–57.
12. Simões, J.M., Levy, J.I., Zaharieva, E.E., Vinson, L.T., Zhao, P., Alpert, M.H., Kath, W.L., Para, A., and Gallio, M. (2021). Robustness and plasticity in *Drosophila* heat avoidance. *Nat. Commun.* **12**, 2044.
13. Wittenburg, N., and Baumeister, R. (1999). Thermal avoidance in *Caenorhabditis elegans*: an approach to the study of nociception. *Proc. Natl. Acad. Sci. USA* **96**, 10477–10482.
14. Edwards, S.L., Charlie, N.K., Milfort, M.C., Brown, B.S., Gravlin, C.N., Knecht, J.E., and Miller, K.G. (2008). A novel molecular solution for ultraviolet light detection in *Caenorhabditis elegans*. *PLoS Biol.* **6**, e198.
15. DeBardleben, H.K., Lopes, L.E., Nessel, M.P., and Raizen, D.M. (2017). Stress-induced sleep after exposure to ultraviolet light is promoted by p53 in *Caenorhabditis elegans*. *Genetics* **207**, 571–582.
16. Davis, K.C., and Raizen, D.M. (2017). A mechanism for sickness sleep: lessons from invertebrates. *J. Physiol.* **595**, 5415–5424.
17. Raizen, D.M., Zimmerman, J.E., Maycock, M.H., Ta, U.D., You, Y.J., Sundaram, M.V., and Pack, A.I. (2008). Lethargus is a *Caenorhabditis elegans* sleep-like state. *Nature* **451**, 569–572.
18. Ohnishi, K., Saito, S., Miura, T., Ohta, A., Tominaga, M., Sokabe, T., and Kuhara, A. (2020). OSM-9 and OCR-2 TRPV channels are accessory warm receptors in *Caenorhabditis elegans* temperature acclimatization. *Sci. Rep.* **10**, 18566.
19. Liu, S., Schulze, E., and Baumeister, R. (2012). Temperature- and touch-sensitive neurons couple CNG and TRPV channel activities to control heat avoidance in *Caenorhabditis elegans*. *PLoS One* **7**, e32360.
20. Liu, J., Ward, A., Gao, J., Dong, Y., Nishio, N., Inada, H., Kang, L., Yu, Y., Ma, D., Xu, T., et al. (2010). *C. elegans* phototransduction requires a G protein-dependent cGMP pathway and a taste receptor homolog. *Nat. Neurosci.* **13**, 715–722.
21. Zhang, W., He, F., Ronan, E.A., Liu, H., Gong, J., Liu, J., and Xu, X.Z.S. (2020). Regulation of photosensation by hydrogen peroxide and antioxidants in *C. elegans*. *PLoS Genet.* **16**, e1009257.
22. Macosko, E.Z., Pokala, N., Feinberg, E.H., Chalasani, S.H., Butcher, R.A., Clardy, J., and Bargmann, C.I. (2009). A hub-and-spoke circuit drives pheromone attraction and social behaviour in *C. elegans*. *Nature* **458**, 1171–1175.
23. Glauser, D.A., Chen, W.C., Agin, R., Macinnis, B.L., Hellman, A.B., Garrity, P.A., Tan, M.W., and Goodman, M.B. (2011). Heat avoidance is regulated by transient receptor potential (TRP) channels and a neuropeptide signaling pathway in *Caenorhabditis elegans*. *Genetics* **188**, 91–103.
24. Choi, S., Taylor, K.P., Chatzigeorgiou, M., Hu, Z., Schafer, W.R., and Kaplan, J.M. (2015). Sensory neurons arouse *C. elegans* locomotion via both glutamate and neuropeptide release. *PLoS Genet.* **11**, e1005359.
25. Busch, K.E., Laurent, P., Soltesz, Z., Murphy, R.J., Faivre, O., Hedwig, B., Thomas, M., Smith, H.L., and de Bono, M. (2012). Tonic signaling from O₂ sensors sets neural circuit activity and behavioral state. *Nat. Neurosci.* **15**, 581–591.

Current Biology

Article



26. Aroian, R.V., Koga, M., Mendel, J.E., Ohshima, Y., and Sternberg, P.W. (1990). The let-23 gene necessary for *Caenorhabditis elegans* vulval induction encodes a tyrosine kinase of the EGF receptor subfamily. *Nature* 348, 693–699.

27. Van Buskirk, C., and Sternberg, P.W. (2007). Epidermal growth factor signaling induces behavioral quiescence in *Caenorhabditis elegans*. *Nat. Neurosci.* 10, 1300–1307.

28. Konietzka, J., Fritz, M., Spiri, S., McWhirter, R., Leha, A., Palumbos, S., Costa, W.S., Orantrh, A., Gottschalk, A., Miller, D.M., et al. (2020). Epidermal growth factor signaling promotes sleep through a combined series and parallel neural circuit. *Curr. Biol.* 30, 1–16.e13.

29. Honer, M., Buscemi, K., Barrett, N., Riazati, N., Orlando, G., and Nelson, M.D. (2020). Orcokinin neuropeptides regulate sleep in *Caenorhabditis elegans*. *J. Neurogenet.* 34, 440–452.

30. Nath, R.D., Chow, E.S., Wang, H., Schwarz, E.M., and Sternberg, P.W. (2016). *C. elegans* stress-induced sleep emerges from the collective action of multiple neuropeptides. *Curr. Biol.* 26, 2446–2455.

31. Nelson, M.D., Lee, K.H., Churgin, M.A., Hill, A.J., Van Buskirk, C., Fang-Yen, C., and Raizen, D.M. (2014). Fmrfamide-like FLP-13 neuropeptides promote quiescence following heat stress in *Caenorhabditis elegans*. *Curr. Biol.* 24, 2406–2410.

32. Turek, M., Besseling, J., Spies, J.P., König, S., and Bringmann, H. (2016). Sleep-active neuron specification and sleep induction require FLP-11 neuropeptides to systemically induce sleep. *eLife* 5, e12499.

33. Steuer Costa, W., Van der Auwera, P., Glock, C., Liewald, J.F., Bach, M., Schüler, C., Wabnig, S., Orantrh, A., Masurat, F., Bringmann, H., et al. (2019). A GABAergic and peptidergic sleep neuron as a locomotion stop neuron with compartmentalized Ca²⁺ dynamics. *Nat. Commun.* 10, 4095.

34. Cianciulli, A., Yoslov, L., Buscemi, K., Sullivan, N., Vance, R.T., Janton, F., Szurgot, M.R., Buerkert, T., Li, E., and Nelson, M.D. (2019). Interneurons regulate locomotion quiescence via cyclic adenosine monophosphate signaling during stress-induced sleep in *Caenorhabditis elegans*. *Genetics* 213, 267–279.

35. Froonckx, L., Van Rompay, L., Temmerman, L., Van Sinay, E., Beets, I., Janssen, T., Husson, S.J., and Schoofs, L. (2012). Neuropeptide GPCRs in *C. elegans*. *Front. Endocrinol. (Lausanne)* 3, 167.

36. Turek, M., Lewandowski, I., and Bringmann, H. (2013). An AP2 transcription factor is required for a sleep-active neuron to induce sleep-like quiescence in *C. elegans*. *Curr. Biol.* 23, 2215–2223.

37. Yuan, J., Zhou, J., Raizen, D.M., and Bau, H.H. (2015). High-throughput motility-based sorter for microswimmers such as *C. elegans*. *Lab Chip* 15, 2790–2798.

38. Iannacone, M.J., Beets, I., Lopes, L.E., Churgin, M.A., Fang-Yen, C., Nelson, M.D., Schoofs, L., and Raizen, D.M. (2017). The RFamide receptor DMSR-1 regulates stress-induced sleep in *C. elegans*. *eLife* 6, e19837.

39. Churgin, M.A., Jung, S.K., Yu, C.C., Chen, X., Raizen, D.M., and Fang-Yen, C. (2017). Longitudinal imaging of *Caenorhabditis elegans* in a microfabricated device reveals variation in behavioral decline during aging. *eLife* 6, e26652.

40. Taylor, S.R., Santpere, G., Weinreb, A., Barrett, A., Reilly, M.B., Xu, C., Varol, E., Oikonomou, P., Glenwinkel, L., McWhirter, R., et al. (2021). Molecular topography of an entire nervous system. *Cell* 184, 4329–4347.e23.

41. Janssen, T., Lindemans, M., Meelkop, E., Temmerman, L., and Schoofs, L. (2010). Coevolution of neuropeptidergic signaling systems: from worm to man. *Ann. N. Y. Acad. Sci.* 1200, 1–14.

42. Zhang, L., Ward, J.D., Cheng, Z., and Dernburg, A.F. (2015). The auxin-inducible degradation (AID) system enables versatile conditional protein depletion in *C. elegans*. *Development* 142, 4374–4384.

43. Ashley, G.E., Duong, T., Levenson, M.T., Martinez, M.A.Q., Johnson, L.C., Hibshman, J.D., Saeger, H.N., Palmisano, N.J., Doonan, R., Martinez-Mendez, R., et al. (2021). An expanded auxin-inducible degron toolkit for *Caenorhabditis elegans*. *Genetics* 217, iyab006.

44. Nishimura, K., Fukagawa, T., Takisawa, H., Kakimoto, T., and Kanemaki, M. (2009). An auxin-based degron system for the rapid depletion of proteins in nonplant cells. *Nat. Methods* 6, 917–922.

45. Trojanowski, N.F., Nelson, M.D., Flavell, S.W., Fang-Yen, C., and Raizen, D.M. (2015). Distinct mechanisms underlie quiescence during two *Caenorhabditis elegans* sleep-like states. *J. Neurosci.* 35, 14571–14584.

46. Ringstad, N., and Horvitz, H.R. (2008). Fmrfamide neuropeptides and acetylcholine synergistically inhibit egg-laying by *C. elegans*. *Nat. Neurosci.* 11, 1168–1176.

47. Nelson, M.D., Janssen, T., York, N., Lee, K.H., Schoofs, L., and Raizen, D.M. (2015). FRPR-4 is a G-protein coupled neuropeptide receptor that regulates behavioral quiescence and posture in *Caenorhabditis elegans*. *PLoS One* 10, e0142938.

48. Puckett Robinson, C., Schwarz, E.M., and Sternberg, P.W. (2013). Identification of DVA interneuron regulatory sequences in *Caenorhabditis elegans*. *PLoS One* 8, e54971.

49. Popovici, C., Isnardon, D., Birnbaum, D., and Roubin, R. (2002). *Caenorhabditis elegans* receptors related to mammalian vascular endothelial growth factor receptors are expressed in neural cells. *Neurosci. Lett.* 329, 116–120.

50. Van Buskirk, C., and Sternberg, P.W. (2010). Paired and LIM class homeodomain proteins coordinate differentiation of the *C. elegans* ALA neuron. *Development* 137, 2065–2074.

51. Yu, Y., Zhi, L., Guan, X., Wang, D., and Wang, D. (2016). FLP-4 neuropeptide and its receptor in a neuronal circuit regulate preference choice through functions of ASH-2 trithorax complex in *Caenorhabditis elegans*. *Sci. Rep.* 6, 21485.

52. Campbell, J.C., Polan-Couillard, L.F., Chin-Sang, I.D., and Bendena, W.G. (2016). NPR-9, a galanin-like G-protein coupled receptor, and GLR-1 regulate interneuronal circuitry underlying multisensory integration of environmental cues in *Caenorhabditis elegans*. *PLoS Genet.* 12, e1006050.

53. Brockie, P.J., Madsen, D.M., Zheng, Y., Mellem, J., and Maricq, A.V. (2001). Differential expression of glutamate receptor subunits in the nervous system of *Caenorhabditis elegans* and their regulation by the homeodomain protein UNC-42. *J. Neurosci.* 21, 1510–1522.

54. Tobin, D.M., Madsen, D.M., Kahn-Kirby, A., Peckol, E.L., Moulder, G., Barstead, R., Maricq, A.V., and Bargmann, C.I. (2002). Combinatorial expression of TRPV channel proteins defines their sensory functions and subcellular localization in *C. elegans* neurons. *Neuron* 35, 307–318.

55. White, J.G., Southgate, E., Thomson, J.N., and Brenner, S. (1986). The structure of the nervous system of the nematode *Caenorhabditis elegans*. *Philos. Trans. R. Soc. Lond. B Biol. Sci.* 314, 1–340.

56. Negishi, T., Kitagawa, S., Horii, N., Tanaka, Y., Haruta, N., Sugimoto, A., Sawa, H., Hayashi, K.I., Harata, M., and Kanemaki, M.T. (2022). The auxin-inducible degron 2 (AID2) system enables controlled protein knockdown during embryogenesis and development in *Caenorhabditis elegans*. *Genetics* 220, iyab218.

57. Cho, J.Y., and Sternberg, P.W. (2014). Multilevel modulation of a sensory motor circuit during *C. elegans* sleep and arousal. *Cell* 156, 249–260.

58. Schwarz, J., Lewandowski, I., and Bringmann, H. (2011). Reduced activity of a sensory neuron during a sleep-like state in *Caenorhabditis elegans*. *Curr. Biol.* 21, R983–R984.

59. Conradt, B., and Horvitz, H.R. (1998). The *C. elegans* protein EGL-1 is required for programmed cell death and interacts with the Bcl-2-like protein CED-9. *Cell* 93, 519–529.

60. Colbert, H.A., Smith, T.L., and Bargmann, C.I. (1997). OSM-9, a novel protein with structural similarity to channels, is required for olfaction, mechanosensation, and olfactory adaptation in *Caenorhabditis elegans*. *J. Neurosci.* 17, 8259–8269.

61. Sokolchik, I., Tanabe, T., Baldi, P.F., and Sze, J.Y. (2005). Polymodal sensory function of the *Caenorhabditis elegans* OCR-2 channel arises from distinct intrinsic determinants within the protein and is selectively conserved in mammalian TRPV proteins. *J. Neurosci.* 25, 1015–1023.

62. Choi, S., Chatzigeorgiou, M., Taylor, K.P., Schafer, W.R., and Kaplan, J.M. (2013). Analysis of NPR-1 reveals a circuit mechanism for behavioral quiescence in *C. elegans*. *Neuron* 78, 869–880.

63. Mellem, J.E., Brockie, P.J., Zheng, Y., Madsen, D.M., and Maricq, A.V. (2002). Decoding of polymodal sensory stimuli by postsynaptic glutamate receptors in *C. elegans*. *Neuron* 36, 933–944.

64. Leonelli, S., Nkambeu, B., and Beaudry, F. (2020). Impaired EAT-4 vesicular glutamate transporter leads to defective nociceptive response of *Caenorhabditis elegans* to noxious heat. *Neurochem. Res.* 45, 882–890.

65. Campbell, S.S., and Tobler, I. (1984). Animal sleep: a review of sleep duration across phylogeny. *Neurosci. Biobehav. Rev.* 8, 269–300.

66. Miyazaki, S., Kawano, T., Yanagisawa, M., and Hayashi, Y. (2022). Intracellular Ca(2+) dynamics in the ALA neuron reflect sleep pressure and regulate sleep in *Caenorhabditis elegans*. *iScience* 25, 104452.

67. Nichols, A.L.A., Eichler, T., Latham, R., and Zimmer, M. (2017). A global brain state underlies *C. elegans* sleep behavior. *Science* 356, eaam6851.

68. Okahata, M., Wei, A.D., Ohta, A., and Kuhara, A. (2019). Cold acclimation via the KQT-2 potassium channel is modulated by oxygen in *Caenorhabditis elegans*. *Sci. Adv.* 5, eaav3631.

69. Jang, H., Kim, K., Neal, S.J., Macosko, E., Kim, D., Butcher, R.A., Zeiger, D.M., Bargmann, C.I., and Sengupta, P. (2012). Neuromodulatory state and sex specify alternative behaviors through antagonistic synaptic pathways in *C. elegans*. *Neuron* 75, 585–592.

70. Dennis, E.J., Dobosiewicz, M., Jin, X., Duvall, L.B., Hartman, P.S., Bargmann, C.I., and Vosshall, L.B. (2018). A natural variant and engineered mutation in a GPCR promote DEET resistance in *C. elegans*. *Nature* 562, 119–123.

71. Sambongi, Y., Nagae, T., Liu, Y., Yoshimizu, T., Takeda, K., Wada, Y., and Futai, M. (1999). Sensing of cadmium and copper ions by externally exposed ADL, ASE, and ASH neurons elicits avoidance response in *Caenorhabditis elegans*. *NeuroReport* 10, 753–757.

72. Troemel, E.R., Chou, J.H., Dwyer, N.D., Colbert, H.A., and Bargmann, C.I. (1995). Divergent seven transmembrane receptors are candidate chemosensory receptors in *C. elegans*. *Cell* 83, 207–218.

73. Ujisawa, T., Ohta, A., Ii, T., Minakuchi, Y., Toyoda, A., Ii, M., and Kuhara, A. (2018). Endoribonuclease ENDU-2 regulates multiple traits including cold tolerance via cell autonomous and nonautonomous controls in *Caenorhabditis elegans*. *Proc. Natl. Acad. Sci. USA* 115, 8823–8828.

74. Zimmerman, J.E., Chan, M.T., Lenz, O.T., Keenan, B.T., Maislin, G., and Pack, A.I. (2017). Glutamate is a wake-active neurotransmitter in *Drosophila melanogaster*. *Sleep* 40, zsw046.

75. John, J., Ramanathan, L., and Siegel, J.M. (2008). Rapid changes in glutamate levels in the posterior hypothalamus across sleep-wake states in freely behaving rats. *Am. J. Physiol. Regul. Integr. Comp. Physiol.* 295, R2041–R2049.

76. Singh, K., Ju, J.Y., Walsh, M.B., Dilorio, M.A., and Hart, A.C. (2014). Deep conservation of genes required for both *Drosophila melanogaster* and *Caenorhabditis elegans* sleep includes a role for dopaminergic signaling. *Sleep* 37, 1439–1451.

77. Chang, A.J., Chronis, N., Karow, D.S., Marletta, M.A., and Bargmann, C.I. (2006). A distributed chemosensory circuit for oxygen preference in *C. elegans*. *PLoS Biol.* 4, e274.

78. Saper, C.B., Chou, T.C., and Scammell, T.E. (2001). The sleep switch: hypothalamic control of sleep and wakefulness. *Trends Neurosci.* 24, 726–731.

79. Maluck, E., Busack, I., Besseling, J., Masurat, F., Turek, M., Busch, K.E., and Bringmann, H. (2020). A wake-active locomotion circuit depolarizes a sleep-active neuron to switch on sleep. *PLoS Biol.* 18, e3000361.

80. Davis, M.W., Somerville, D., Lee, R.Y., Lockery, S., Avery, L., and Fambrough, D.M. (1995). Mutations in the *Caenorhabditis elegans* Na,K-ATPase alpha-subunit gene, eat-6, disrupt excitable cell function. *J. Neurosci.* 15, 8408–8418.

81. Stiernagle, T. (2006). Maintenance of *C. elegans*. *WormBook*, 1–11. <https://doi.org/10.1895/wormbook.1.101.1>.

82. Kutscher, L.M., and Shaham, S. (2014). Forward and reverse mutagenesis in *C. elegans*. *WormBook* 2014, 1–26.

83. Nelson, M.D., and Fitch, D.H. (2011). Overlap extension PCR: an efficient method for transgene construction. *Methods Mol. Biol.* 772, 459–470.

84. Kim, K., and Li, C. (2004). Expression and regulation of an fmrfamide-related neuropeptide gene family in *Caenorhabditis elegans*. *J. Comp. Neurol.* 475, 540–550.

85. Hori, S., Oda, S., Suehiro, Y., Iino, Y., and Mitani, S. (2018). OFF-responses of interneurons optimize avoidance behaviors depending on stimulus strength via electrical synapses. *PLoS Genet.* 14, e1007477.

86. Paix, A., Folkmann, A., and Seydoux, G. (2017). Precision genome editing using CRISPR-Cas9 and linear repair templates in *C. elegans*. *Methods* 121–122, 86–93.

87. Dokshin, G.A., Ghanta, K.S., Piscopo, K.M., and Mello, C.C. (2018). Robust genome editing with short single-stranded and long, partially single-stranded DNA donors in *Caenorhabditis elegans*. *Genetics* 210, 781–787.

88. Ghanta, K.S., and Mello, C.C. (2020). Melting dsDNA donor molecules greatly improves precision genome editing in *Caenorhabditis elegans*. *Genetics* 216, 643–650.

89. Yu, C.C., Raizen, D.M., and Fang-Yen, C. (2014). Multi-well imaging of development and behavior in *Caenorhabditis elegans*. *J. Neurosci. Methods* 223, 35–39.

90. Hart, and Anne C., eds. (2006). Behavior *WormBook*, The *C. elegans* Research Community (*WormBook*). <https://doi.org/10.1895/wormbook.1.87.1>. <http://www.wormbook.org>.

STAR★METHODS

KEY RESOURCES TABLE

REAGENT or RESOURCE	SOURCE	IDENTIFIER
<i>C. elegans</i> strains		
Bristol - <i>wild type</i>	CGC	N2
<i>osm-9</i> (ky10)IV	CGC	CX10
<i>ocr-2</i> (ak47)IV	CGC	VM396
<i>pha-1</i> (e2132ts)III; <i>syEx723</i> [<i>hsp-16.2p::lin-3C</i> ; <i>myo-2p::gfp</i> ; <i>pha-1</i> (+)]	Van Buskirk and Sternberg ²⁷	PS5009
<i>qnls226</i> [<i>hsp-16.2p::nlp-14</i> ; <i>myo-2p::mCherry</i>]	Honer et al. ²⁹	SJU241
<i>stj327</i> ; <i>qnls226</i>	This study	SJU327
<i>stj328</i> ; <i>qnls226</i>	This study	SJU328
<i>stj329</i> ; <i>qnls226</i>	This study	SJU329
<i>stj330</i> ; <i>qnls226</i>	This study	SJU330
<i>npr-38</i> (<i>stj330</i>)X	This study	SJU353
<i>stjEx226</i> [<i>npr-38</i> (++); <i>myo-2p::gfp</i>]	This study	SJU360
<i>stjEx227</i> [<i>npr-38</i> (++); <i>myo-2p::gfp</i>]	This study	SJU361
<i>F59B2.13</i> (<i>stj374</i>)	This study	SJU376
<i>npr-38</i> (<i>stj367</i>)X	This study	SJU378
<i>nlp-14</i> (<i>stj18</i>)X; <i>stjEx227</i>	This study	SJU381
<i>npr-38</i> (<i>stj367</i>); <i>stjEx235</i> [<i>twk-16p(cs1)</i> :: <i>pes-1p::npr-38</i> ; <i>myo-2p::mCherry</i>]	This study	SJU384
<i>npr-38</i> (<i>stj367</i>); <i>stjEx234</i> [<i>twk-16p(cs1)</i> :: <i>pes-1p::npr-38</i> ; <i>myo-2p::mCherry</i>]	This study	SJU396
<i>stjEx245</i> [<i>flp-11p::npr-38</i> ; <i>myo-2p::mCherry</i>]	This study	SJU398
<i>npr-38</i> (<i>stj367</i>)X; <i>stjEx246</i> [<i>flp-11p::npr-38</i> ; <i>myo-2p::mCherry</i>]	This study	SJU399
<i>npr-38</i> (<i>stj367</i>)X; <i>stjEx245</i> [<i>flp-11p::npr-38</i> ; <i>myo-2p::mCherry</i>]	This study	SJU402
<i>ceh-17</i> (<i>np1</i>)I; <i>aptf-1</i> (<i>gk794</i>)II; <i>stjEx227</i> [<i>npr-38</i> (++); <i>myo-2p::gfp</i>]	This study	SJU404
<i>nlp-14</i> (<i>stj18</i>)X; <i>nlp-15</i> (<i>ok1512</i>)I; <i>stjEx227</i> [<i>npr-38</i> (++); <i>myo-2p::gfp</i>]	This study	SJU405
<i>npr-38</i> (<i>stj367</i>)X; <i>syEx723</i>	This study	SJU411
<i>npr-38</i> (<i>stj367</i>)X; <i>stjEx247</i> [<i>ver-3p::npr-38</i> ; <i>myo-2p::mCherry</i>]	This study	SJU412
<i>npr-38</i> (<i>stj367</i>)X; <i>stjEx248</i> [<i>ver-3p::npr-38</i> ; <i>myo-2p::mCherry</i>]	This study	SJU416
<i>stjEx250</i> [<i>npr-38</i> (+); <i>myo-2p::gfp</i>]	This study	SJU417
<i>stjEx251</i> [<i>npr-38</i> (+); <i>myo-2p::gfp</i>]	This study	SJU418
<i>stjEx252</i> [<i>npr-38</i> (+); <i>myo-2p::gfp</i>]	This study	SJU419
<i>ceh-14</i> (<i>ch3</i>)X; <i>stjEx227</i> [<i>npr-38</i> (++); <i>myo-2p::gfp</i>]	This study	SJU421
<i>aptf-1</i> (<i>gk794</i>)II; <i>stjEx227</i> [<i>npr-38</i> (++); <i>myo-2p::gfp</i>]	This study	SJU422

(Continued on next page)

Continued

REAGENT or RESOURCE	SOURCE	IDENTIFIER
<i>npr-38(stj367)X; stjEx247 [glr-8p::npr-38; myo-2p::mCherry]</i>	This study	SJU430
<i>npr-38(stj367)X; stjEx248 [glr-8p::npr-38; myo-2p::mCherry]</i>	This study	SJU431
<i>npr-38(stj367)X; stjEx251[npr-38(+); myo-2p::gfp]</i>	This study	SJU432
<i>npr-38(stj367)X; stjEx275[srh-220p::npr-38; myo-2p::mCherry]</i>	This study	SJU453
<i>npr-38(stj452)X</i>	This study	SJU457
<i>npr-38(stj367)X; stjEx278[srh-220p::npr-38; myo-2p::mCherry]</i>	This study	SJU460
<i>npr-38(stj367)X; stjEx279[srh-220p::npr-38; myo-2p::mCherry]</i>	This study	SJU461
<i>npr-38(stj367)X; stjEx282[npr-9p::npr-38; myo-2p::mCherry]</i>	This study	SJU464
<i>npr-38(stj367)X; stjEx283[npr-9p::npr-38; myo-2p::mCherry]</i>	This study	SJU465
<i>npr-38(stj367)X; stjEx291[flp-11p::npr-38; myo-2p::mCherry]</i>	This study	SJU476
<i>flp-21(ok889)V; stjEx227[npr-38(++)</i> <i>myo-2p::gfp]</i>	This study	SJU481
<i>nlp-8(syb762)I; stjEx227[npr-38(++)</i> <i>myo-2p::gfp]</i>	This study	SJU482
<i>stjEx296[srh-220p::egl-1; myo-2p::mCherry]</i>	This study	SJU487
<i>npr-38(stj452)X; stjEx305[eft-3p::tir1; myo-2p::mCherry]</i>	This study	SJU497
<i>npr-38(stj452)X; stjEx308[twk-16p(cs1)::pes-1p::tir1; myo-2p::mCherry]</i>	This study	SJU500
<i>npr-38(stj452)X; stjEx312[srh-220p::tir1; myo-2p::mCherry]</i>	This study	SJU504
<i>npr-38(stj367)X; stjEx317[sra-6p::npr-38; myo-2p::mCherry]</i>	This study	SJU514
<i>npr-38(stj367)X; stjEx318[sra-6p::npr-38; myo-2p::mCherry]</i>	This study	SJU515
<i>npr-38(stj367)X; stjEx320[ocr-2p::npr-38; myo-2p::mCherry]</i>	This study	SJU517
<i>npr-38(stj367)X; stjEx321[ocr-2p::npr-38; myo-2p::mCherry]</i>	This study	SJU518
<i>npr-38(stj367)X; stjEx323[flp-21p::npr-38; myo-2p::mCherry]</i>	This study	SJU520
<i>npr-38(stj367)X; stjEx324[flp-21p::npr-38; myo-2p::mCherry]</i>	This study	SJU521
<i>npr-38(stj367); stjEx296[srh-220p::egl-1; myo-2p::mCherry]</i>	This study	SJU525
<i>stjEx327[nlp-50(+); myo-2p::mCherry]</i>	This study	SJU527
<i>stjEx328[nlp-50(+); myo-2p::mCherry]</i>	This study	SJU528
<i>npr-38(stj367)X; nlp-14(stj18)X</i>	This study	SJU530
<i>stjEx330[srh-220p::ChannelRhodopsin2::mCherry; myo-2p::gfp]</i>	This study	SJU534
<i>stjEx334[srh-220p::npr-38 (high copy), myo-2p::mCherry]</i>	This study	SJU537
<i>stjEx335[srh-220p::npr-38 (high copy), myo-2p::mCherry]</i>	This study	SJU538

(Continued on next page)

Continued

REAGENT or RESOURCE	SOURCE	IDENTIFIER
<i>nlp-50</i> (stj553)II	This study	SJU553
<i>nlp-50</i> (stj553)II; <i>stj347</i> [<i>srh-220p::nlp-50</i> , <i>myo-2p::mCherry</i>]	This study	SJU556
Bacterial strain		
<i>Escherichia coli</i>	Davis et al. ⁸⁰	DA837
Oligonucleotides		
Sequence	Description	Identifier, primer pair
CAACAAATCGTATTTTCAC	<i>npr-38p::gfp</i> 6kb 5' of <i>npr-38</i>	oSJU703, oSJU705
GATATTTTACATTGACGCAC	<i>npr-38p::gfp</i> Nested to 703	oSJU704, oSJU129
AAACACCCAGTATTGCCAAGAATGGG AACATGACTCACAACTCAATGCGAG	<i>npr-38p::gfp</i> -1 to <i>npr-38</i> and adds a <i>gfp</i> complementary tail	oSJU705, oSJU703
AGAATACTCGCATTGAGTTGTGAGTA CATGAGTAAAGGAGAAGAACCTTTC	<i>npr-38p::gfp</i> +1 to <i>gfp</i> and adds a <i>npr-38</i> complementary tail	oSJU706, oSJU128
GAGGGAGCACAAATTTCG	<i>npr-38p::gfp</i> 3' of the <i>unc-54</i> 3'UTR in pPD95.75 (addgene©)	oSJU89, oSJU706
GAATCTACACAATTTCATTGTTAGAGG	<i>npr-38p::gfp</i> Nested to oSJU128	oSJU90, oSJU704
CTGAAATCTCTTTCATTGCTC	Overexpression and genomic rescue	oSJU707, oSJU703
CTAGTTTGCATTTCGCATTG	<i>ver-3p::npr-38</i> 4.5kb 5' of <i>ver-3</i>	oSJU739, oSJU741
GCATTTCGCATTGTATTGATCTC	<i>ver-3p::npr-38</i> Nested to oSJU739	oSJU740, oSJU722
CCAGTATTGCCAAGAATGGGACATC AATTCATCTCAGAAAAATTGTTC	<i>ver-3p::npr-38</i> -1 to <i>ver-3</i> and adds a <i>npr-38</i> complementary tail	oSJU741, oSJU739
ACAAGAACAAATTTCCTGAGATGAAATT GATGTTCCCATTCTGGCAATAC	<i>ver-3p::npr-38</i> +1 to <i>npr-38</i> and adds a <i>ver-3</i> complementary tail	oSJU742, oSJU707
CTTTTCATTGCTCGTAAACGTC	<i>ver-3p::npr-38</i> Nested to oSJU707	oSJU722, oSJU740
CAACATACTGCACAAATGGAC	<i>fip-11p::npr-38</i> 4kb 5' of <i>fip-11</i>	oSJU731, oSJU733
CATACTGCACAAATGGACTC	<i>fip-11p::npr-38</i> Nested to oSJU731	oSJU732, oSJU722
AGTATTGCCAAGAATGGGACATTGAG TCATTATTCACTATGAAC	<i>fip-11p::npr-38</i> -1 to <i>fip-11</i> and adds a <i>npr-38</i> complementary tail	oSJU733, oSJU731
TTGCAGTTCACTGAATAATGACTCAA TGTTCCCATTCTGGCAATAC	<i>fip-11p::npr-38</i> +1 to <i>npr-38</i> and adds a <i>fip-11</i> complementary tail	oSJU734, oSJU707
CAATGATCAGTATTGCACTCTC	<i>glr-8p::npr-38</i> 4.5kb 5' of <i>glr-8</i>	oSJU817, oSJU733
GATCAGTATTGCACTCTCAATTAG	<i>glr-8p::npr-38</i> Nested to oSJU817	oSJU818, oSJU722
ACCCAGTATTGCCAAGAATGGGACATTCC TTTCATTCGGAAAGCGAAAG	<i>glr-8p::npr-38</i> -1 to <i>glr-8</i> and adds a <i>npr-38</i> complementary tail	oSJU819, oSJU731
AACACTTTCGCTTCGAAATGAAAGGAAT GTTCCCATTCTGGCAATAC	<i>glr-8p::npr-38</i> +1 to <i>npr-38</i> and adds a <i>glr-8</i> complementary tail	oSJU820, oSJU707

(Continued on next page)

Continued

REAGENT or RESOURCE	SOURCE	IDENTIFIER
CATGCCAGGCAAGCTATTAC	<i>npr-9p::npr-38</i> 3kb 5' of <i>npr-9</i>	oSJu912, oSJu819
GTAGCAGAAATCCAAATCCAAAC	<i>npr-9p::npr-38</i> Nested to oSJu817	oSJu913, oSJu722
ACACCCAGTATTGCCAAGAATGGGAACATT	<i>npr-9p::npr-38</i>	oSJu914, oSJu912
TCCATTGTCAAAAGTTGATG	-1 to <i>npr-9</i> and adds a <i>npr-38</i> complementary tail	
TGAAATCATCAACTTTGACAATGGAAATG	<i>npr-9p::npr-38</i>	oSJu915, oSJu707
TTCCCATTCTGGCAATAC	+1 to <i>npr-38</i> and adds a <i>npr-9</i> complementary tail	
GACTAACGTGCTATGGTCATTC	<i>srh-220p::npr-38</i> 2kb 5' of <i>srh-220</i>	oSJu875, oSJu877
GTCTTAGTCCGAATTTGTGAG	<i>srh-220p::npr-38</i> Nested to oSJu875	oSJu876, oSJu722
ACACCCAGTATTGCCAAGAATGGGAACATA	<i>srh-220p::npr-38</i>	oSJu877, oSJu875
GTCATACTTGAGTTGGACCC	-1 to <i>srh-220</i> and adds a <i>npr-38</i> complementary tail	
TGGCTTTCGGTCCAAACTCAAGTATGACTA	<i>srh-220p::npr-38</i>	oSJu878, oSJu707
TGTTCCCATTCTGGCAATAC	+1 to <i>npr-38</i> and adds a <i>srh-220</i> complementary tail	
AAATAAAATAATTCTAGACTTACCAAGCATACT	<i>srh-220p::egl-1</i>	oSJu936, oSJu875
TGAGTTGGACCGAAAAG	-1 to <i>srh-220</i> and adds a <i>egl-1</i> complementary tail	
GCTGGCTTTCGGTCCAAACTCAAGTA	<i>srh-220p::egl-1</i>	oSJu937, oSJu938
TGCTGGTAAGTCTAGAAATTATT	+1 to <i>egl-1</i> and adds a <i>srh-220</i> complementary tail	
CTCTAGTATGAATCGATATTGAG	<i>srh-220p::egl-1</i> 3' of <i>egl-1</i>	oSJu938, oSJu937
CTAGTATGAATCGATATTGAGTTGTC	<i>srh-220p::egl-1</i> Nested to oSJu938	oSJu839, oSJu876
CTGTCATGGTCAGTATTGAGAAG	<i>sra-6p::npr-38</i> 4kb 5' of <i>sra-6</i>	oSJu975, oSJu977
CATGGTCAGTATTGAGAAGAAG	<i>sra-6p::npr-38</i> Nested to oSJu975	oSJu976, oSJu722
TCTTGATGTCATGCCCTCCCAGATGCA	<i>sra-6p::npr-38</i> -1 to <i>sra-6</i> and adds a <i>npr-38</i> complementary tail	oSJu977, oSJu975
TGGCAAAATCTGAAATAATAAATA		
ATTTAATTTATTATTCAGATTTGCCAT	<i>sra-6p::npr sra-6 -38</i> +1 to and adds a <i>npr-38</i> complementary tail	oSJu978, oSJu707
GACTATGGGAGGCATGAC		
CTCTCTGAAACTTACCTCCCTAG	<i>fip-21p::npr-38</i> 5.7kb 5' of <i>fip-21</i>	oSJu996, oSJu1000
GTTTGACACAACGTAAACGATATT	<i>fip-21p::npr-38</i> Nested to oSJu975	oSJu997, oSJu722
ACCCAGTATTGCCAAGAATGGGAACATCG	<i>fip-21p::npr-38</i>	oSJu1000, oSJu996
TCTGAAAATGACTTTGGA	-1 to <i>fip-21</i> and adds a <i>npr-38</i> complementary tail	
TCCAAAATCCAAAAAGTCATTTCAGACGA	<i>fip-21p::npr-38</i> +1 to <i>npr-38</i> and adds a <i>fip-21</i> complementary tail	oSJu1001, oSJu707
TGTTCCCATTCTGGCAATAC		
AACGCTCGTAATTGCAAAAAATCGATCGA	<i>twk-16(cs1)p::pes-10p::npr-38</i> 3' of <i>cs1</i> enhancer and adds a <i>pes-10</i> complementary tail	oSJu199, oSJu201
TGCTTGCAACAAGGCAA		

(Continued on next page)

Continued

REAGENT or RESOURCE	SOURCE	IDENTIFIER
TCTTTTGCCTTGTGCAAAGCATCGATCGA TTTTTGCAAAATTACGAG	<i>twk-16(cs1)p::pes-10p::npr-38</i> 5' of <i>pes-10</i> and adds a <i>cs1</i> complementary tail	oSJU200, oSJU723
GACTAAGCTGGCTAACAGTTGC	<i>twk-16(cs1)p::pes-10p::npr-38</i> +1kb to <i>cs1</i> enhancer of <i>twk-16</i>	oSJU201, oSJU199
GCTAAGTTGCAAGTTCATC	<i>twk-16(cs1)p::pes-10p::npr-38</i> Nested to oSJU201	oSJU202, oSJU722
AGTATTGCCAAGAATGGGAAACATCTGAAAG TTAAAAATTACAGTATAAAG	<i>twk-16(cs1)p::pes-10p::npr-38</i> 3' of <i>pes-10</i> and adds a <i>npr-38</i> complementary tail	oSJU723, oSJU200
ATCTTATACTGTAATTTAACCTTCAGATG TTCCCATTCTGGCAATAC	<i>twk-16(cs1)p::pes-10p::npr-38</i> +1 to <i>npr-38</i> and adds a <i>pes-10</i> complementary tail	oSJU724, oSJU707
GTTCCCTAACGACACTGCGAAC	<i>ocr-2p::npr-38</i> 4kb 5' of <i>ocr-2</i>	oSJU963, oSJU965
GACACTGCGAAACTCATAACTG	<i>ocr-2p::npr-38</i> Nested to oSJU963	oSJU964, oSJU722
TTGTATGTCATGCCCTCCCATAGTCATCTAA TGATGTGATGACTCTACTG	<i>ocr-2p::npr-38</i> -1 to <i>ocr-2</i> and adds a <i>npr-38</i> complementary tail	oSJU965, oSJU963
TTATCAGTAGAGTACATCACATCATTAAAGATGA CTATGGGAGGCGATGAC	<i>ocr-2p::npr-38</i> +1 to <i>npr-38</i> and adds a <i>ocr-2</i> complementary tail	oSJU966, oSJU707
TGGAAACGACAAGGCGATTCTCTTTGCATAG TCATACTTGAGTTGGACC	<i>srh-220p::tir1</i> Binds -1 to <i>srh-220</i> and adds a <i>tir1</i> complementary tail	oSJU879, oSJU875
TGGCTTTCGGCCAAACTCAAGTATGACTAT GCAAAAGAGAACATGCCCTG	<i>srh-220p::tir1</i> Binds +1 to <i>tir1</i> in pTN4 and adds a <i>srh-220</i> complementary tail	oSJU880, oSJU838
CAGCAGAATTCAAAGCAAAAGAC	<i>srh-220p::tir1</i> Binds 3' of the <i>unc-54</i> 3'UTR in pTN4	oSJU838, oSJU880
GCATCGGTAGTCATATTGATCTG	<i>srh-220p::tir1</i> Nested to oSJU838	oSJU839, oSJU876
AACGACAAGGCGATTCTCTTTGCATCTGAAA GTTAAAAATTACAGTATAAAG	<i>twk-16(cs1);pes-10p::tir1</i> Binds -1 to <i>pes-10</i> and adds a <i>tir1</i> complementary tail	oSJU853, oSJU200
TCCCTTATCTTATACTGTAATTTAACCTTC GATGAAAAGAGAACATGCCCTG	<i>twk-16(cs1);pes-10p::tir1</i> Binds +1 to <i>tir1</i> and adds a <i>pes-10</i> complementary tail	oSJU854, oSJU838
TGTCAAATGTTGAAAGATTGGAG	<i>nlp-50</i> overexpression Binds 5' of <i>nlp-50</i>	oSJU1004, oSJU1005
TGATAATGGCATACTTCTGTGG	<i>nlp-50</i> overexpression Binds 3' of <i>nlp-50</i>	oSJU1005, oSJU1004
ACGGCAGACAAAGCGCCGCCATAGT CCATACTTGAGTTGGACCGAAAAG	<i>srh-220p::ChR2</i> Binds -1 to <i>srh-220</i> and adds a <i>ChR2</i> complementary tail	oSJU922, oSJU875
TGAGCTGGCTTTCGGTCCAAACTCAA GTATGGACTATGGCGCGCTTG	<i>srh-220p::ChR2</i> Binds +1 to <i>ChR2</i> in the addgene plasmid 117420	oSJU923, oSJU920
CAGTTATGTTGGTATATTGGGAATG	<i>srh-220p::ChR2</i> Binds 3' of the <i>unc-54</i> 3'UTR in the addgene plasmid 117420	oSJU920, oSJU923
GTTTGGTATATTGGGAATGTATTCTG	<i>srh-220p::ChR2</i> Nested to oSJU920	oSJU921, oSJU876

(Continued on next page)

Continued

REAGENT or RESOURCE	SOURCE	IDENTIFIER
AAATAGAGCAACAAAGACGGAGAAGCG CATAGTCATACTTGAGTTGGAC	<i>srh-220p::nlp-50</i> Binds -1 to <i>srh-220</i> and adds a <i>nlp-50</i> complementary tail	oSJU1037, oSJU875
TTTCGGTCCAAACTCAAGTATGACTAT GCGCTCTCCGTCTTGTT	<i>srh-220p::nlp-50</i> +1 to <i>nlp-50</i> and adds a <i>srh-220</i> complementary tail	oSJU1038, oSJU1005
CATACTTCTGTGGGCCTTAAG	<i>srh-220p::nlp-50</i> 3' of <i>nlp-50</i>	oSJU1039, oSJU876
CRISPR oligos		
Sequence	Description	Identifier
ACTGTTCTCACGATTGAATGCGG	Guide RNA for <i>stj367</i>	oSJUcrRNA18
ACATTCAGATAACCCAGAGAGAAAAATGTG CATCGGAATATCATAGCTAGCATAGCATGT GGTTTGAGTTACAAACATCATCTAGCTT TTCTTGCA	Repair template for <i>stj367</i>	oSJUcrDNA112
GTATGGTCCAATCAGTTGAG	Forward screening for <i>stj367</i>	oSJUcrDNA113
CTGTTATCTCAATATTTCCATCTG	Reverse screening for <i>stj367</i>	oSJUcrDNA114
CGTAATTCTCCCCATTCAA	Guide RNA for AID-GFP insertion of <i>npr-38</i>	oSJUcrRNA19
ACTAAAGCATTCAAAGGTTCAGATTCA GATCCCTCCCTGAAACATCATTGGCG ATTCAAGTAACAACCTGTTCTACAGTAT GCCTAAAGATCCAGCCAAAC	Forward – AID-GFP with Long homology arm for <i>npr-38</i>	oSJUcrDNA133
TTAAAACAATTCCGGCCTAATTCTTAAAG TCTAATGCATTGGAGAAAATGACATAAA TGGAACGCCGCATTCATCATTGAAAGTT CATCCATT	Reverse – AID-GFP with Long homology arm for <i>npr-38</i>	oSJUcrDNA134
TCATTGGCGATTCAAGTAACAACCTGTTCTC ACGATATGCCTAAAGATCCAGCCAAAC	Forward – AID-GFP with Short homology arm for <i>npr-38</i>	oSJUcrDNA135
TTTGAGAAAATGACATAATGGAACGCCGC ATTCACTATTGAAAGTTCATCCATT	Reverse – AID-GFP with Short homology arm for <i>npr-38</i>	oSJUcrDNA136
ACAGTAAACATTCGCAAAGAAATG	Forward screening for AID-GFP	oSJU873
GATTTCACGTTCTGTGAAATGTCG	Reverse screening for AID-GFP	oSJU874
ACTGTTCTCACGATTGAATGCGG	Guide RNA for F59B2.13	oSJUcrRNA20
TGCTTGTGCTGAAAGCTTTTGATG GCACACAATACCACGTGTAGGCTAGCTA GGCTTGTGGATTGATTCCGAACGT TGGTCCGGAATGA	Repair template for <i>stj374</i>	SJUcrDNA119
GAATTCGTCTATAGAATGTTAGCTG	Forward screening for <i>stj374</i>	SJUcrDNA120
GACGTAGGAACGTGAGAAATGTGAC	Reverse screening for <i>stj374</i>	SJUcrDNA121
CTATCTTCAGCAGTCACAGC	Guide RNA for <i>nlp-14</i>	oSJUcrRNA1
TCGTTCTCTAGTTGCCCTATCTCAGC AGTCACATGCTAGCAGCCGGTAAGTT ATTGAACGTATCATGAAAAC	Repair template for <i>stj18</i>	oSJUcrDNA3
CTTTGTGACTCACTGATTTTC	Forward screening for <i>stj18</i>	oSJUcrDNA1
CACTGTACTTTCGACTAGTTGC	Reverse screening for <i>stj18</i>	oSJUcrDNA2
GCTCTCTTGTGCTCTTATGG	Guide RNA for <i>nlp-50</i>	oSJUcrRNA22
CTTCCAACGCCCTTGTCTCAC	Forward screening for <i>stj553</i>	oSJUcrDNA153
GTCTGCTGGGTATTCTCCTAC	Reverse screening for <i>stj553</i>	oSJUcrDNA154
Software and algorithms		
MATLAB (version R2019a)	Churgin et al. ³⁹	Mathworks
BioRender	BioRender	biorender.com
GraphPad Prism	GraphPad by Dotmatics	graphpad.com/scientific-software/prism/

RESOURCE AVAILABILITY

Lead contact

Further information and requests for resources and reagents should be directed to and will be fulfilled by the lead contact, Matthew D Nelson (mnelson@sju.edu).

Materials availability

Requests for strains should be directed to the [lead contact](#).

Data and code availability

- All data reported in this paper will be shared by the [lead contact](#) upon request.
- This paper does not report original code.
- Any additional information required to reanalyze the data reported in this paper is available from the [lead contact](#) upon request.

EXPERIMENTAL MODEL AND SUBJECT DETAILS

Animals were maintained at 20°C on agar plates containing nematode growth medium and fed the OP50 derivative bacterial strain DA837.⁸⁰ All transgenic strains used in this study are listed in the [key resources table](#).

METHOD DETAILS

Genetic screen

Worm-ramp devices were made on a PRUSAi3 3D-printer using polylactic acid filament material with the following dimensions (LxWxH): 4x1x1.5cm. Worm-ramps were composed of a pitched 18-degree channel containing 1mm longitudinal scallops along the bottom to provide greater traction for the worms, separating a lower loading chamber and an upper collection platform^{37,38} (Figure S1). 1000-2000 *nlp-14* overexpressing animals (Strain: SJU241) were synchronized by using an egg-preparation protocol⁸¹ and allowed to grow to the L4/young adult stage. These animals were exposed to 5µM ethyl methanesulfonate (EMS) diluted in M9 buffer and incubated at room temperature for 4 h.⁸² Mutagenized worms were evenly distributed and grown on seeded agar plates and allowed to produce progeny. Another egg-preparation was performed on the F1 generation to collect the F2 eggs, which were then plated and grown to adulthood. The F2 animals were washed into 15ml conical tubes containing M9 buffer and placed in a 33° Celsius water bath for 30 min. 2 h post-heat shock, the worms were transferred to the loading chamber of the worm-ramp and screened. Once loaded into the bottom chamber, the animals were allowed to swim, if possible, for 10–15 min. Animals that reached the top collection platform were isolated using a glass pipette and singled onto seeded agar plates and grown to the F3 generation. These animals underwent secondary behavioral screening that included manual counting of body bends, and WorMotel analyses.

Molecular biology and transgenesis

DNA for transgenesis was constructed using the overlap extension-polymerase chain reaction (OE-PCR).⁸³ Constructs for cell-specific rescue were made by first amplifying the genomic promoter sequence of the genes *ver-3* (ALA),^{49,50} *flp-11* (RIS),³² *gtr-8* (I6),⁵³ *flp-21* (RMG),⁸⁴ a defined enhancer (*cs1*) of *twk-16* (DVA),⁴⁸ *npr-9* (AIB),⁵² *srh-220* (ADL),¹⁸ *sra-6* (ASH), and *ocr-2* (ADL+ASH).⁵⁴ The *cs1* enhancer was fused to the *pes-10* basal promoter, which was amplified from the Fire vector L3135 (Addgene©). Each promoter was fused to the coding sequence and 3'UTR of *npr-38*, which was amplified from genomic DNA, by OE-PCR. The *npr-38* transcriptional reporter was made by fusing the 5' region upstream of *npr-38* (5816bp), amplified from genomic DNA, and the *gfp* coding sequence, including *unc-54* 3'UTR, from the Fire vector pPD95.75 (Addgene©). To express *tir1* in the ADL and DVA neurons, the *srh-220* promoter and *twk-16*(*cs1*) enhancer elements were fused to the *tir1* coding and *unc-54* 3'UTR sequence, amplified from pTN4 (Addgene ©), by OE-PCR. To express *tir1* in all cells, pTN4 was injected directly.⁵⁶ To express channel rhodopsin-2 (ChR2) in the ADL neurons, the *srh-220* promoter was fused to the coding sequence of ChR2(H134R) followed by the sequence for mCherry, which was amplified from the addgene© plasmid 117420.⁸⁵ To express *nlp-50* in the ADL neurons, the *srh-220* promoter was fused to the genomic sequence of *nlp-50* by OE-PCR. All oligonucleotides used in this study are listed in the [key resources table](#).

Construction of mutants

The *stj330* allele of *npr-38* was identified following whole genome sequencing (GeneWiz©). This strain was outcrossed to N2 (3X) to generate the strain SJU353. The *stj367* (strain SJU378), and *stj452* (strain SJU457) insertion alleles of *npr-38*, the *stj374* insertion allele of F59B12.13 (strain SJU376), the *npr-38*(*stj367*);*nlp-14*(*stj18*) double mutants, and the *nlp-50*(*stj553*) mutant were constructed by CRISPR/Cas9 gene editing, using defined protocols.⁸⁶ For *stj367* and *stj374*, a single-stranded oligo was designed which contained 35bp homology arms flanking three stop codons in distinct reading frames and a NheI restriction site (NEB©). For the

AID-GFP insertion, described strategies to improve gene insertion efficiency were employed.^{87,88} Briefly, the AID-GFP sequence was PCR amplified from pLZ29 (addgene©),⁴² under two different conditions. In one reaction, primers with short 35bp homology arms (oSJUcrDNA135 and oSJUcrDNA136) were used, and in a second reaction primers with long >80bp homology arms (oSJUcrDNA133 and oSJUcrDNA134) were used. The two pcr products were purified using a NucleoSpin Gel and PCR Cleanup, mini-kit (Macherey-Nagel ©), and then melted together in equimolar concentration, using a described protocol.^{87,88} For each CRISPR mutant, an edit of the *dpv-10* gene was made simultaneously, to allow for screening.⁸⁶ Specifically, a mixture of guide RNA (gRNA) duplexed with Alt-R® CRISPR-Cas9 tracrRNA (IDT ©), Alt-R® S.p. Cas9 Nuclease V3 (IDT), and oligonucleotide repair templates (*stj367*, *stj374*), or melted PCR products were injected into day-1 adult wild-type (N2) animals. For the *npr-38(stj367);nlp-14(stj18)* double mutants, previously described reagents,²⁹ were injected into *npr-38(stj367)* mutants to generate the *stj18* insertion allele of *nlp-14*. This approach was used in place of a genetic cross because both genes are on chromosome X. To identify the CRISPR mutants, F1 dumpy and/or roller animals were singled from each injection, allowed to self, and screened by PCR followed by restriction digest. If necessary, the resultant mutants were crossed with N2 to remove the *dpv-10* mutations. For the *nlp-50(stj553)* strain, the mutation was identified randomly by screening for a band smaller than controls using gel electrophoresis. All reagents are listed in the [key resources table](#).

WorMotel behavioral assays

Movement quiescence was quantified during both developmentally timed sleep and stress induced sleep, using the WorMotel, as previously described.³⁹ For stress-induced sleep, L4 animals were picked to freshly seeded plates the day prior to the experiment. Day-1 adults were transferred to the surface of the agar, loaded into a 24-welled PDMS microchip. For UV-induced stress-induced sleep analyses, the chip was placed into a UV-cross linker (Ultraviolet, 254 UVP) and exposed to 1500 J/m² of UV light, as described.¹⁵ For heat-induced stress-induced sleep, the chip was placed in a petri-dish wrapped with parafilm and submerged in a water bath set at 37°C for 30 min. For all mutant analyses, wild-type animals were run concurrently with mutants over multiple trials, which were then averaged. For rescue experiments, wild-type, mutant, and rescued strains were run on the same chip over multiple trials. A minimum of two transgenic lines were analyzed for each rescued strain. To measure developmentally-timed sleep, the same protocol was followed, but animals were placed on the microchip during the mid-L4 stage and allowed to develop to young adulthood. Quiescence was quantified as previously described.^{39,89} Total movement quiescence in 8 h, also referred to as sleep (min) in 8 h, was compared across multiple trials of the relevant comparison using Student's t-test (wild type vs. mutant) or one-way ANOVA followed by Tukey's multiple comparisons test (wild type vs. mutant vs. rescued/transgenic strain). Sleep duration was determined by measuring the time of a sleep bout, which was identified as a period of time in which the movement quiescence was above 0.5 min in a 10-min window, and was sustained for at least 20 min, similar to previous studies.¹⁷ Average sleep duration was compared using Student's t-test (wild type vs. mutant).

Avoidance and body bending analyses

To quantify activity manually, we counted body bends over a 1-min span in day-1 adult animals, using a stereomicroscope. A body bend was defined as one movement in either direction, in which the head changed direction, as previously described.⁹⁰ The average number of bends were calculated and compared across genotypes using one-way ANOVA followed by Tukey's multiple comparisons test.

For blue-light avoidance assays, body bends were quantified in day-1 adult animals every minute for 5 min, under constant blue light, using a Leica MZ50 fluorescent dissecting microscope (magnification=50X). For heat avoidance assays, body bends were counted for 1 min on room temperature plates, at which point worms were manually transferred, by picking, to another room temperature plate and body bends were counted again. Next, worms were transferred to pre-warmed 35°C plates and body bends were quantified again. The plates were allowed to cool to room temperature for 30 min and bends were again quantified. The average number of bends were calculated and compared across conditions using one-way ANOVA followed by Tukey's multiple comparisons test.

Optogenetic experiments

The transgenic strain SJU534 was used for all optogenetic experiments. First-day adult animals expressing ChR2 in the ADL neurons were transferred to plates seeded with DA837 bacteria alone or plates seeded with DA837 supplemented with 10µg/ml ATR (Retinol solution, Cerilliant®). Animals were allowed to acclimate to these plates for a minimum of 4 h. Single adults were then exposed to blue light using a Leica MZ50 fluorescent dissecting microscope (magnification=50X) for 1 min and body bends were quantified, as described above. This was done before stress (pre-stress) and 15, 30, 45, 60, 75, 90, and 120 min after UV shock. Average body bends were compared between ATR and no-ATR at each time-point using Student's t-test.

For sleep analyses, first-day adult animals expressing ChR2 in the ADL neurons were transferred to plates seeded with DA837 bacteria alone or plates seeded with DA837 supplemented with 10µg/ml ATR (Retinol solution, Cerilliant®), for 4 h. Animals were then transferred to the agar surface of a 24-welled PDMS microchip seeded with DA837 alone (12 wells) or with ATR (12 wells). The entire chip was placed into a UV-cross linker (Ultraviolet, 254 UVP) and exposed to 1500 J/m² of UV light, and then imaged in a WorMotel for 8 h. During this time, the entire chip was exposed to blue light using a LED light strip (Wentop ©) every 15 min for 2 h.

Quiescence during heat exposure

Quiescence during heat exposure was quantified by manually observing worms on standard growth plates that were placed on a slide warmer set at 37°C for 30 min. The number of animals moving was counted every minute and the fraction of animals quiescent was calculated by dividing the number of quiescent worms by the total number of worms. This was repeated over a minimum of 5 trials. The fraction of quiescence was compared between genotypes using two-way ANOVA followed by Sidak's multiple comparisons test.

Microscopy

Fluorescence microscopy was conducted using an Olympus BX63 wide-field fluorescence microscope equipped with a Hamamatsu FLASH 4.0V3 digital camera and CellSens Dimension Version 2 software. Day-1 adult transgenic animals were immobilized on glass slides containing a 5% agar pad supplemented with 25mM sodium azide.

QUANTIFICATION AND STATISTICAL ANALYSES

Statistical significance was calculated using GraphPad Prism 9 software. The details of all statistical tests can be found in the figure legends. Statistical parameters such as sample size (N=number of animals) and p-values can also be found in the figure legends. Unless otherwise noted in the legend, data is presented as means and error bars represent SEM.